

Table of Contents

Part I SCET 2019 Conference Schedule.....	3
Part II Plenary Speeches	4
Engineering Mathematics and Physics.....	4
Plenary Speech 1: AI Based Simulation and Analysis by Malliavin Calculus for Backward Stochastic Partial Differential Equations.....	4
Plenary Speech 1: Advances on some graph theory problems - a survey.....	4
Plenary Speech 3: Neutrosophic extended triplet groups and applications.....	5
Plenary Speech 4: High-Performance Thermally Activated Delayed Fluorescence Polymers for Efficient Electroluminescence.....	6
Plenary Speech 5: Performance Analysis of Hopfield Neural Networks as Associative Memory for Fingerprint Images.....	7
Plenary Speech 6: A model based on fuzzy inference system to analyze the trends of financial market ..	9
Material, Chemical & Mineral Processing/Metallurgical Engineering	10
Plenary Speech 1: Mechanical behavior of beta-type titanium alloy porous scaffolds produced by additive manufacturing	10
Plenary Speech 2: Ideal Flow Theory for Metal Forming Design.....	11
Plenary Speech 3: Hydration and Adsorption Phenomena of Biopolymers in Heterogeneous Solid-Liquid Systems.....	11
Plenary Speech 4: Nano Powders Produced and Utilized as Additives Drop-in Process Technology to Upgrade Commercial Polyolefins	12
Plenary Speech 5: Interfacial Structure and Functional Properties of Complex Oxide Heterojunctions..	13
Plenary Speech 6: Implementation of Water and Waste Minimization in Companies.....	13
Plenary Speech 7: Microwave Metallurgy.....	14
Plenary Speech 8: Use of Electro-Fenton Process for Treating Petroleum Wastewater	15
Plenary Speech 9: Functional Fabrics with Special Wettabilities	16
Part III Technical Sessions	17
Engineering Mathematics and Physics: Plenary Speech II & Technical Session	17
Material, Chemical & Mineral Processing/Metallurgical Engineering: Technical Session I: Oral Presentations	18
Material, Chemical & Mineral Processing/Metallurgical Engineering: Technical Session II: Poster Presentations	19
Part IV Abstracts.....	24

Part V Instructions for Presentations42
Part VI Hotel Information43
Contact Us44

Part I SCET 2019 Conference Schedule

Time: April 22-24, 2019

Location: Ramada Xiamen Hotel (厦门华美达长升大酒店)

Date	Time	Lobby, Ramada Xiamen Hotel	
April 22	14:00-17:00	Registration	
Date	Time	Conference Room II (彩虹厅)	Conference Room V (荣泰阁)
April 23	08:30-11:30	Engineering Mathematics and Physics: Plenary Speech Session I Prof. Wanyang Dai, Prof. Chunhui Lai, Prof. Choonkil Park, Prof. Guohua Xie Chair: Prof. Wanyang Dai Coffee Break & Group Photo: 10:00-10:15	Material, Chemical & Mineral Processing/Metallurgical Engineering: Plenary Speech Session I Prof. Laichang Zhang, Dr. Sergei Alexandrov, Prof. Lee D. Wilson, Prof. Haiping Chen Chair: Prof. Laichang Zhang Coffee Break & Group Photo: 10:00-10:15
	11:30-13:30	Lunch [旭园餐厅 Chinese Restaurant, 2 nd Floor]	
	Time	Conference Room II (彩虹厅)	Conference Room V (荣泰阁)
	14:00-17:00	Engineering Mathematics and Physics: Plenary Speech Session II & Technical Session Dr. Manu Pratap Singh, Dr. Sanjeev Kumar Chair: Coffee Break & Group Photo: 16:00-16:15	Material, Chemical & Mineral Processing/Metallurgical Engineering: Plenary Speech Session II Prof. Hossein Ganjidoust, Dr. BITA AYATI, Prof. Guo Chen, Prof. Yan Zhao Chair: Coffee Break & Group Photo: 16:00-16:15
17:30-19:30	Dinner [旭园餐厅 Chinese Restaurant, 2 nd Floor]		
Date	Time	Conference Room V (荣泰阁)	
April 24	08:30-11:30	Material, Chemical & Mineral Processing/Metallurgical Engineering: Technical Session 1: Oral Presentations Chair: Dr. Ramesh Subramanian Coffee Break & Group Photo: 10:00-10:15	Material, Chemical & Mineral Processing/Metallurgical Engineering: Technical Session 1I: Poster Presentations Coffee Break & Group Photo: 10:00-10:15
	11:30-13:30	Lunch [旭园餐厅 Chinese Restaurant, 2 nd Floor]	
April 25	07:00-19:00	One Day Tour (pending, on own expense)	

Part II Plenary Speeches

Engineering Mathematics and Physics

Plenary Speech 1: AI Based Simulation and Analysis by Malliavin Calculus for Backward Stochastic Partial Differential Equations

Speaker: Prof. Wanyang Dai, Nanjing University, China

Time: 08:30-09:15, Tuesday Morning, April 23, 2019

Location: Conference Room II (彩虹厅), the 3rd Floor, Ramada Xiamen Hotel



Abstract

We develop a generic convolution neural network (CNN) based scheme to simulate the 2-tuple adapted strong solution in a classical sense to a generalized Cauchy (or called terminal-value) problem, i.e., to a unified system of stochastic partial differential equations (B-SPDEs including infinite-dimensional B-SDEs) driven by Brownian motions. The scheme consists of two convolution parts: W layers of backward networks and L layers of reinforcement iterations. More importantly, it is a completely discrete and iterative algorithm in terms of both time and space with mean-square convergence supported by both theoretical proof and numerical examples. In doing so, the system is assumed to be high-dimensional and vector-valued, whose drift and diffusion coefficients may involve nonlinear and high-order partial differential operators. Under general local Lipschitz and linear growth conditions, the unique existence of the 2-tuple adapted strong solution to the system is proved by constructing a suitable Banach space to handle the difficulty that the partial differential orders on both sides of these equations are different. During the proof, we also develop new techniques of random field Malliavin calculus to show the unique existence of 2-tuple adapted strong solutions to two embedded systems of the first-order and second-order Malliavin derivative based B-SPDEs under random environments.

Plenary Speech 1: Advances on some graph theory problems - a survey

Speaker: Prof. Chunhui Lai, Minnan Normal University, China

Time: 09:15-10:00, Tuesday Morning, April 23, 2019

Location: Conference Room II (彩虹厅), the 3rd Floor, Ramada Xiamen Hotel



Abstract

Hajós conjectured that every simple even graph on n vertices can be decomposed into at most $\frac{n}{2}$ cycle (see L.Lovasz, On covering of graphs, in: P. Erdos, G. O. H. Katona (Eds.), Theory of Graphs, Academic Press, New York, 1968, pp. 231-236). Gallai conjectured that every simple connected graph on n vertices can be decomposed into at most $\frac{n+1}{2}$ paths (see L. Lovasz, On covering of graphs, in: P. Erdos, G.O.H. Katona (Eds.), Theory of Graphs, Academic Press, New York, 1968, pp. 231-236). In 1976, Thomassen C. conjectures that every longest cycle in a 3-connected graph has a chord (see Bondy J. A., Murty U. S. R., Graph theory, Graduate Texts in Mathematics, 244, Springer, New York, 2008, Unsolved Problems 65). Given a graph H , what is the maximum number of edges of a graph with n vertices not containing H as a subgraph? This number is denoted $ex(n, H)$, and is known as the Turan number. P. Erdos conjectured that there exists a positive constant c such that $ex(n, C_{2k}) \geq cn^{1+1/k}$ (see P. Erdos, Some unsolved problems in graph theory and combinatorial analysis, Combinatorial Mathematics and its Applications (Proc. Conf., Oxford, 1969), pp. 97-109, Academic Press, London, 1971). R. C. Entringer raised the problem of determine which simple graphs G have exactly one cycle of each length l , $3 \leq l \leq v$ (see J.A. Bondy and U.S.R. Murty, Graph Theory with Applications (Macmillan, New York, 1976), p. 247, Problem 10). Let $f(n)$ be the maximum number of edges in a graph on n vertices in which no two cycles have the same length. P. Erdos raised the problem of determining $f(n)$ (see J.A. Bondy and U.S.R. Murty, Graph Theory with Applications (Macmillan, New York, 1976), p. 247, Problem 11). We present the problems, conjectures related to these problems and we summarize the know results. We do not think Hajós conjecture is true.

Plenary Speech 3: Neutrosophic extended triplet groups and applications

Speaker: Prof. Choonkil Park, Hanyang University, Republic of Korea

Time: 10:15-11:00, Tuesday Morning, April 23, 2019

Location: Conference Room II (彩虹厅), the 3rd Floor, Ramada Xiamen Hotel

Abstract

Celik, Shalla and Olgun defined neutro-homomorphisms in neutrosophic extended triplet groups and Zhang et al. investigated neutro-homomorphisms



in neutrosophic extended triplet groups. In this note, we apply the results on neutro-homomorphisms in neutrosophic extended triplet groups to investigate C^* -algebra homomorphisms in unital C^* -algebras. Assume that A is a unital C^* -algebra with multiplication operation \star , unit e and unitary group $U(A)$ and that B is a unital C^* -algebra with multiplication operation \star and unitary group $U(B)$.

Definition 1. Let $(U(A), \star)$ and $(U(B), \star)$ be unitary groups of unital C^* -algebras A and B , respectively. A mapping $h: U(A) \rightarrow U(B)$ is called a neutro- $*$ -homomorphism if $h(u\star v) = h(u)\star h(v)$, $h(u^*) = h(u)^*$ for all u, v in $U(A)$.

We obtain the following main result.

Theorem 1. Let A and B be unital C^* -algebras. Let $H: A \rightarrow B$ be a complex-linear mapping and let $h: (U(A), \star) \rightarrow (U(B), \star)$ be a neutro- $*$ -homomorphism. If $H|_{U(A)} = h$, then $H: A \rightarrow B$ is a C^* -algebra homomorphism.

Further, we introduce and solve bi-additive functional inequalities and prove the Hyers-Ulam stability of the bi-additive functional inequalities in complex Banach spaces. This is applied to investigate b -derivations on C^* -algebras, Lie C^* -algebras and JC^* -algebras, and derivations on C^* -algebras, Lie C^* -algebras and JC^* -algebras associated with the bi-additive functional inequalities. Moreover, we study biderivations on C^* -ternary algebras and C^* -triple systems associated with the bi-additive functional inequalities.

Plenary Speech 4: High-Performance Thermally Activated Delayed Fluorescence

Polymers for Efficient Electroluminescence

Speaker: Dr. Guohua Xie, Wuhan University, China

Time: 11:00-11:45, Tuesday Morning, April 23, 2019

Location: Conference Room II (彩虹厅), the 3rd Floor, Ramada Xiamen Hotel



Abstract

Light-emitting polymers featuring thermally activated delayed fluorescence (TADF) characteristics are attracting intensive interests in terms of developing low-cost and large-area light-emitting devices for practical applications in flat-panel displays and solid-state lighting. Due to the efficient reverse intersystem crossing process, TADF polymers can theoretically generate and utilize 100% of the excitons under electrical excitation. A series of bluish-green TADF polymers grafting the TADF moiety onto the side chain of the polymer backbone of polycarbazole were developed, resulting in 63.7% exciton utilization ratio under electroluminescence process. To further improve the performances, another series of bluish-green TADF polymers were synthesized via side-chain strategy, which completely inherited the TADF features of the side-chain TADF unit. Through the complicated fluorescence sensitization, the optimal device reached a considerably high external quantum efficiency of 16.1%, i.e. nearly

85% of the electrically generated excitons were utilized for light emission,. Finally, we designed a series of orange-red TADF polymers with a backbone-donor/pendant-acceptor structure with a PLQY up to 99%, and demonstrated highly efficient red TADF polymer based OLEDs with an EQE up to 19.4%, i.e., nearly 98% utilization ratio of the singlet and triplet excitons under EL process. By managing the incomplete energy transfer between the backbone and the orange-emitting TADF unit, the single-molecule white TADF polymer was demonstrated with high brightness.

Reference

- [1] J. Luo, G. Xie, S. Gong, T. Chen, and C. Yang, *Chemical Communications*, 2016, 52, 2292.
- [2] G. Xie, J. Luo, M. Huang, T. Chen, K. Wu, S. Gong, and C. Yang, *Advanced Materials*, 2017, 29, 1604223.
- [3] Y. Wang, Y. Zhu, G. Xie, H. Zhan, C. Yang, and Y. Cheng, *Journal of Materials Chemistry C*, 2017, 5, 10715.

Plenary Speech 5: Performance Analysis of Hopfield Neural Networks as Associative Memory for Fingerprint Images

Speaker: Prof. Manu Pratap Singh, Dr. B. R. Ambedkar University, India

Time: 14:00-14:45, Tuesday Afternoon, April 23, 2019

Location: Conference Room II (彩虹厅), the 3rd Floor, Ramada Xiamen Hotel



Abstract

Pattern recognition is a dominant research area in the field of Machine intelligence. Pattern recognition is considered with various techniques of soft computing. In different approaches of soft computing the pattern recognition is considered as the non constraint multi objective optimization problem. Pattern storage & recalling i.e. pattern association is one of prominent method for the pattern recognition task that one would like to realize using an artificial neural network (ANN) as associative memory feature. Pattern storage is generally accomplished by a feedback network consisting of processing units with non-linear bipolar output functions. The stable states of the network represent the memorized or stored patterns. Since the Hopfield neural network with associative memory was introduced, various modifications are developed for the purpose of storing and retrieving memory patterns as fixed-point attractors. The dynamics of these networks have been studied extensively because of their potential applications. The dynamics determines the retrieval quality of the associative memories corresponding to already stored patterns. The pattern information in an unsupervised manner is encoded as sum of correlation weight matrices in the connection strengths between the preceding units of feedback neural network using the locally available information of the pre and post synaptic units which is considered as final or parent weight matrix.

Hopfield proposed a fully connected neural network model of associative memory in which we can store information by distributing it among neurons, and recall it from the dynamically relaxed neuron states. If we map these states corresponding to certain desired memory vectors, then the time

evolution of dynamics leads to a stable state. These stable states of the networks represent the stored patterns. Hopfield used the Hebbian learning rule to prescribe the weight matrix for establishing these stable states. A major drawback of this type of neural networks is that the memory attractors are constantly accompanied with a huge number of spurious memory attractors so that the network dynamics is very likely to be trapped in these attractors, and thereby prevents the retrieval of the memory attractors. Hopfield type networks also likely are trapped in non-optimal local minima close to the starting point, which is not desired. The presence of false minima will increase the probability of error in recall of the stored pattern. The problem of false minima can be reduced by adopting the evolutionary algorithm to accomplish the search for global minima. There have been a lot of researchers who apply evolutionary techniques (simulated annealing and Genetic algorithm) to minimize the problem of false minima. Imades & Akira have applied evolutionary computation to Hopfield neural networks in various ways. A rigorous treatment of the capacity of the Hopfield associative memory can be found in. The Genetic algorithm has been identified as one of prominent search technique for exploring the global minima in Hopfield neural network.

Developed by Holland, a Genetic algorithm is a biologically inspired search technique. In simple terms, the technique involves generating a random initial population of individuals, each of which represents a potential solution to a problem. Each member of this population evaluates from a fitness function which is selected against some known criteria. The selected members of the population from the fitness function are used to generate the new population as the members of the population are then selected for reproduction based potential solutions from the operations of the genetic algorithm. The process of evaluation, selection, and recombination is iterated until the population converges to an acceptable optimal solution. Genetic algorithms (GAs) require only fitness information, not gradient information or other internal knowledge of a problem as in case of neural networks. Genetic algorithms have traditionally been used in optimization but, with a few enhancements, can perform classification, prediction and pattern association as well. The GA has been used very effectively for function optimization and it can perform efficient searching for approximate global minima. It has been observed that the pattern recalling in the Hopfield type neural networks can be performed efficiently with GA. The GA in this case is expected to yield alternative global optimal values of the weight matrix corresponding to all stored patterns. The conventional Hopfield neural network suffers from the problem of non-convergence and local minima on increasing the complexity of the network. However, GA is particularly good to perform efficient searching in large and complex space to find out the global optima and for convergence. Considerable research into the Hopfield network has shown that the model may trap into four types of spurious attractors. Four well identified classes of these attractors are mixture states, spin glass states, compliment states and alien attractors. As the complexity of the of the search space increases, GA presents an increasingly attractive alternative for pattern storage & recalling in Hopfield type neural networks of associative memory.

The neural network applications address problems in pattern classification, prediction, financial analysis, and control and optimization. In most current applications, neural networks are best used as aids to human decision makers instead of substitutes for them. Genetic algorithms have helped market researchers performing market segmentation analysis. Genetic algorithms and neural networks can be integrated into a single application to take advantage of the best features of these technologies.

Much work has been done on the evolution of neural networks with GA. There have been a lot of

researches which apply evolutionary techniques to layered neural networks. However, their applications to fully connected neural networks remain few so far. The first attempt to conjugate evolutionary algorithms with Hopfield neural networks dealt with training of connection weights and design of the neural network architecture, or both. Evolution has been introduced in neural networks at three levels: architectures, connection weights and learning rules. The evolution of connection weights proceeds at the lowest level on the fastest time scale in an environment determined by architecture, a learning rule, and learning tasks. The evolution of connection weights introduces an adaptive and global approach to training, especially in the reinforcement learning and recurrent network learning paradigm. Training of neural networks using evolutionary algorithms started in the beginning of 90's . Reviews can be found in. Cardenas et al. presented the architecture optimization of neural networks using parallel genetic algorithms for pattern recognition based on person faces. They compared the results of the training stage for sequential and parallel implementations. The genetic evolution has been used as data structures processing for image classification.

The work on which we are focusing due to its scientific importance and socially relevancy is to analyze the performance of a Hopfield neural network for storage and recall of fingerprint images. The study implements a form of unsupervised learning. Here first we discuss the storage and recall via hebbian learning and the problem areas or the efficiency issues involved and then the performance enhancement via the pseudo-inverse learning. Performance is measured with respect to storage capacity; recall of distorted or noisy patterns i.e. association of a noisy version of a stored pattern to the original stored pattern for testing the accretive behavior of the network and association of new or noisy / distorted patterns to some stored pattern.

Plenary Speech 6: A model based on fuzzy inference system to analyze the trends of financial market

Speaker: Prof. Sanjeev Kumar, Dr. B.R. Ambedkar University, India

Time: 14:45-15:30, Tuesday Afternoon, April 23, 2019

Location: Conference Room II (彩虹厅), the 3rd Floor, Ramada Xiamen Hotel



Abstract

Stock investment has become an important investment activity and the internet makes it easier to exchange stock information and to make stock transactions. Trading system in stock market is full of uncertainty therefore nobody can make accurate decision for investing their money and therefore investors often lose money due to unclear investment objective. Predicting the stock market is very difficult since it depends on several unknown factors. Technical analysis is sometimes used in financial markets to assist traders to make buying and selling decision. This work will examine a trading model that combines fuzzy logic and technical analysis to find patterns and trends in financial market. To accomplish this goal, the daily data of a financial institute from July 2012 to June 2013 is used. Here take four input factors and use fuzzy logic to find the output. For fuzzifying these input data, trapezoidal membership function is used, and center of gravity method is used for defuzzification of fuzzy output. Finally, observed that

this fuzzy logic model gives best result to put on hold with degree of precision 37.587%.

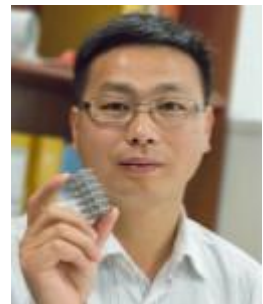
Material, Chemical & Mineral Processing/Metallurgical Engineering

Plenary Speech 1: Mechanical behavior of beta-type titanium alloy porous scaffolds produced by additive manufacturing

Speaker: Prof. Laichang Zhang, Edith Cowan University, Australia

Time: 08:30-09:15, Tuesday Morning, April 23, 2019

Location: Conference Room V (荣泰阁), the 3rd Floor, Ramada Xiamen Hotel



Abstract

Beta-type titanium porous structures are a new class of solution for implants because they offer excellent combination of high strength and low Young's modulus. This presentation studies the influence of porosity variation in electron beam melting (EBM)-produced and selective laser melting (SLM) produced beta-type titanium alloy samples on the mechanical properties including super-elastic property, Young's modulus, compression strength, energy absorption and fatigue properties. Compared with Ti-6Al-4V samples, the beta-type titanium porous samples exhibit a higher normalized fatigue strength owing to super-elastic property, greater plastic zone ahead of the fatigue crack tip and the crack deflection behaviour. Stress distribution results, obtained by finite element methods, coupled with the investigation of the slip bands generated have been used to reveal the plasticity mechanism and local stress concentrations for each structure. The topology optimized structure exhibits the best balance of bending and buckling stress with a high elastic energy absorption, a low Young's modulus and a high compression strength.

References:

01. Y.J. Liu, S.J. Li, H.L. Wang, W.T. Hou, Y.L. Hao, R. Yang, T.B. Sercombe, and L.C. Zhang*, Microstructure, defects and mechanical behavior of beta-type titanium porous structures manufactured by electron beam melting and selective laser melting. *Acta Materialia*, Vol. 113, pp. 56-67 (2016). (ESI Highly Cited Paper)
02. Y.J. Liu, H.L. Wang, S.J. Li, S.G. Wang, W.J. Wang, W.T. Hou, Y.L. Hao, R. Yang, and L.C. Zhang*, Compressive and fatigue behavior of beta-type titanium porous structures fabricated by electron beam melting. *Acta Materialia*, Vol. 126, pp. 58-66 (2017). (ESI Highly Cited Paper)
03. Y.J. Liu, S.J. Li, L.C. Zhang*, Y.L. Hao, and T.B. Sercombe, Early plastic deformation behaviour and energy absorption in porous β -type biomedical titanium produced by selective laser melting. *Scripta Materialia*, Vol. 153, pp. 99-103 (2018).
04. L.C. Zhang*, Y.J. Liu, S.J. Li, and Y.L. Hao, Additive manufacturing of titanium alloys by electron beam melting: A review. *Advanced Engineering Materials*, Vol. 20, No. 5, paper No. 1700842 (2018) (Invited review paper)

Plenary Speech 2: Ideal Flow Theory for Metal Forming Design

Speaker: Prof. Sergei Alexandrov, Beihang University, China

Time: 09:15-10:00, Tuesday Morning, April 23, 2019

Location: Conference Room V (荣泰阁), the 3rd Floor, Ramada Xiamen Hotel



Abstract

Ideal flows have been defined elsewhere as solenoidal smooth deformations in which an eigenvector field associated everywhere with the greatest principal strain rate is fixed in the material. Under such conditions all material elements undergo paths of minimum plastic work, a condition which is advantageous for metal forming processes. The ideal flow theory has been used as the basis of a procedure for the preliminary design of such processes. In particular, the distribution of strain and material properties is uniform in the final product of steady processes. The ideal flow theory has been long associated with the Tresca yield criterion and its associated flow rule. The objective of the present paper is to extend this theory to the double shearing model and the double slip and rotation model that are widely adopted in pressure – dependent plasticity. Both steady and nonsteady processes under plane strain and axial symmetry conditions are considered. Efficient numerical approaches for design of metal forming processes are developed. The approaches are based on the method of characteristics. In the case of plane strain problems, the original system of equations reduces to the equation of telegraphy and subsequent numerical integration.

Plenary Speech 3: Hydration and Adsorption Phenomena of Biopolymers in Heterogeneous Solid-Liquid Systems

Speaker: Dr. Lee D. Wilson, University of Saskatchewan, Canada

Time: 10:15-11:00, Tuesday Morning, April 23, 2019

Location: Conference Room V (荣泰阁), the 3rd Floor, Ramada Xiamen Hotel



Abstract

Molecular selective adsorption processes at the solid surface of biopolymers in mixed solvent systems are poorly understood due to manifold interactions. However, the ability to achieve adsorptive fractionation of liquid mixtures is posited to relate to role of specific solid-liquid interactions at the adsorbent interface. The hydration of solid biopolymers (starch, cellulose, etc.) in binary aqueous systems is partly governed by the relative solvent binding affinities with the biopolymer surface sites, in accordance with the role of textural and surface chemical properties. While molecular models that account for surface area and solvent effects provide reliable estimates of hydration energy and binding affinity parameters, spectroscopic and thermodynamic methods offer a facile alternative experimental approach to

account for detailed aspects of solvation phenomena at biopolymer interfaces during adsorption. In this presentation, thermal and spectroscopic methods were used to gain insight on the interaction of starch- and cellulose-based materials in neat and binary water-ethanol (W-E) mixtures. Batch adsorption studies in binary W-E mixtures reveal the selective solvent uptake properties by the biomaterials, in agreement with their solvent swelling in pure water or ethanol. The nature, stability of the bound water and the thermodynamic properties of the biopolymers in variable hydration states were probed via differential scanning calorimetry (DSC) and Raman spectroscopy. The trends in biopolymer-solvent interactions are supported by dye adsorption and scanning electron microscopy (SEM) results, further indicating that biopolymer adsorption properties in W-E mixtures strongly depend on the surface area, pore structure, and accessibility of the polar surface groups of the biopolymer systems, in line with solvent selective uptake results reported herein.

Plenary Speech 4: Nano Powders Produced and Utilized as Additives Drop-in Process Technology to Upgrade Commercial Polyolefins

Speaker: Prof. Haiping Chen, AMERICA P&G CO., USA

Time: 11:00-11:45, Tuesday Morning, April 23, 2019

Location: Conference Room V (荣泰阁), the 3rd Floor, Ramada Xiamen Hotel



Abstract

#Our USA Team offer Technology transfer to produce New Nano powders

#Upgrade conventional plastics or rubber to new Nano high-end products

applied in aerospace, transportation, energy, construction, and explosion-proof safety

#A Drop-in Technology: New Nano powders can be mixed a small ratio with reactor resins or additives in plastic or rubber existing production lines

#Successful experience applied for USA Companies and China-US joint company

#Upgrade Commodity and Specialty Poleolefins / Plastics on Major Technical Indicators included:

Extra high mechanical strength, increased corrosion and chemical resistance, high wear abrasion resistance, higher pressure, higher temperature, and lower temperature resistance

#Upgrade Rubber products used in tires, etc. on major technical indicators included: high mechanical strength and high abrasion wear resistance

#Nano sizes of silicon carbide (SiC) and Nano sizes of alumina produced by our USA Patented process technology

#A Drop-in Process Technology of Nano powders to existing production lines

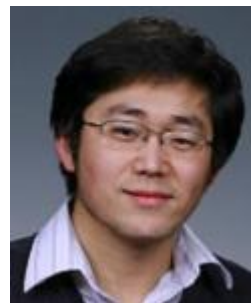
#Upgrade major technical indicators mainly included: superior mechanical strength, excellent chemical corrosion resistance, high abrasion wear strength, higher temperature and lower temperature resistance

Plenary Speech 5: Interfacial Structure and Functional Properties of Complex Oxide Heterojunctions

Speaker: Prof. Liang Qiao, University of Electronic Science and Technology of China

Time: 11:45-12:30, Tuesday Morning, April 23, 2019

Location: Conference Room V (荣泰阁), the 3rd Floor, Ramada Xiamen Hotel



Abstract

Due to delicate balance among crystal structure, chemical composition and electronic configurations, bulk perovskite complex oxides have demonstrated a broad range of electronic, magnetic and optical functional properties. Recent advance in thin-film fabrication and characterization techniques have further made it possible for precise control of material synthesis and perfecting their properties for important information technology and energy-related applications. The most exciting part of oxide thin-film research lies in the fact that it offers extra degrees of freedoms to tune the functionalities, e.g. epitaxial strain, interface formation, and crystal symmetry mismatch, which are not available in their bulk form.

In this talk, I will be focusing on the inter-correlations among epitaxial film growth, interface structure, and induced (electronic and magnetic) properties of perovskite oxide heterojunctions. Driven by chemical solubility and inherent polar discontinuity, these material systems are prevented from forming structurally coherent and chemically abrupt interfaces, as demonstrated by state-of-art spectroscopy and microscopy techniques. Intermixing of the cations at interfaces is demonstrated to result in dramatic change of electronic structure and electrical behaviors for $\text{LaAlO}_3/\text{SrTiO}_3$ and $\text{LaCrO}_3/\text{SrTiO}_3$. In addition to intermixing, the interfacial symmetry-mismatch is shown to surpass the traditional lattice mismatch to stabilize novel interfacial states with unique octahedral structure and spin configuration. The symmetry breaking at $\text{LaCoO}_3/\text{SrTiO}_3$ interface dramatically modifies the structure of fundamental CoO_6 building-blocks. The combination of epitaxial strain and octahedral tilting results in pronounced $t_{2g}^* \rightarrow e_g$ spin-transition and a microscopic long-range magnetic ordering in LaCoO_3 , which doesn't have this property in bulk phase.

Plenary Speech 6: Implementation of Water and Waste Minimization in

Companies

Speaker: Prof. Hossein Ganjidoust, Tarbiat Modares University, Iran

Time: 14:00-14:45, Tuesday Afternoon, April 23, 2019

Location: Conference Room V (荣泰阁), the 3rd Floor, Ramada Xiamen Hotel



Abstract

Iran, is one of the countries located in a dry and semi-dry area. Many provinces are facing water scarcity. This is not only due to the low rates of precipitation

received, but also because of the increase in demand on water resources for municipal, agricultural and industrial uses. For reduction of water consumption, many research works have been carried out. Wastewater reuse has proven to be effective and successful in creating a new reliable water supply. The present study aim to propose an overview on the water productivity and wastewater minimization in industries which consumes a great amount of water in different units. In this paper some industries were chosen to measure the possibilities of decrease in water consumption and reduction in wastewater production. The management system implemented in the companies resulted in up to 50% save in water in addition to reduction in materials used for the production. Recover of useful materials from the wastewater, recycle and reuse of wastewater in the plant and overall of large amount of wastewater which was minimized have been resulted in the companies. At the end, some suggestions have been given for implementing the water and wastewater minimization plan in the companies.

Key Words: Water Productivity, Minimization, Wastewater, Reuse

Plenary Speech 7: Microwave Metallurgy

Speaker: Prof. Guo Chen, Kunming University of Science and Technology, Kunming, P.R. China

Time: 14:45-15:30, Tuesday Afternoon, April 23, 2019

Location: Conference Room V (荣泰阁), the 3rd Floor, Ramada Xiamen Hotel



Abstract

Microwave metallurgy is a new metallurgy technology which has been developed recently and now is an attractive advanced inter-disciplinary field.

Taking advantages of microwave heating, it is possible to develop new metallurgy technique and process, which cannot be realized under conventional heating method, reforming some traditional metallurgy process and technology, upgrading deep-processing level of metallurgical products, improving the product structure and finally achieving the efficient, energy-saving, and environmental-friendly metallurgical process. It can be expected that the development of microwave metallurgy will play an increasingly important role in the future metallurgical technology, so the microwave metallurgy is included in the application guides for both National Science Foundations and 'Eleven-Five' 863 plans (National High Technology Research and Development Program).

Within the research fields, (i) The temperature-rising properties of many ores in microwave field have been measured; the temperature rising equations have been derived and calculated; the temperature rising process has been quantized and finally data of several ores' temperature rising characteristics have been acquired. (ii) Microwave drying of various kinds of metallurgical ores and metallurgical chemical products have been performed; microwave calcining of various kinds of metallurgical intermediate products has been performed, and thermodynamics and kinetics of the reaction system and process for metallurgical reduction and leaching under microwave fields have been studied. Thus, the following research areas have been formed:

- ① New technologies of microwave drying
- ② New technologies of microwave calcining
- ③ New technologies of microwave-intensification oxidation- reduction
- ④ New technologies of microwave-intensification leaching
- ⑤ Other new technologies of microwave metallurgy
- ⑥ Theories of the interaction between microwave field and metallurgical materials

Plenary Speech 8: Use of Electro-Fenton Process for Treating Petroleum

Wastewater

Speaker: Prof. BITA AYATI, Tarbiat Modares University, Iran

Time: 15:45-16:30, Tuesday Afternoon, April 23, 2019

Location: Conference Room V (荣泰阁), the 3rd Floor, Ramada Xiamen Hotel



Abstract

Petroleum industry is the most important industry in Iran. The wastewater generated in different units would include many various compounds depending on reactions complexity and refined materials. Application of electrochemical reactors, electro-flotation, adsorption, microwave-assisted oxidation and biological methods for treatment of petroleum wastewater encounters with different operational issues and problems like incomplete remediation and sidelong generation of toxic compounds. Moreover, biological treatment methods used for industrial wastewater treatment are usually less robust systems in comparison to electrochemical methods with special regards to toxicity usually found in petroleum wastewater and the risk of odor problems exists as well. Advanced oxidation treatment methods have drawn great attention for their great potential in different industrial wastewater treatment. Hydroxyl radical is produced in all advanced oxidation processes, and although unselective this radical is able to degrade organics in a short time. H₂O₂ and ferrous ions released by iron electrodes corrosion are used to generate hydroxyl radicals in Electro-Fenton method.

In this study, treatment of a 750 mL petroleum wastewater sample was evaluated using a sequential hybrid system which was consisted of Electro-Fenton and NZVI slurry reactors. In both systems, effective parameters were optimized by OFAT method considering energy consumption and treatment efficiency. As for the slurry reactor, nanoparticles were first synthesized and then used in the reactor to treat the wastewater. Both systems were first optimized separately and the hybrid complex was designed considering the sub-systems optimum conditions. As for the Electro-Fenton reactor, COD removal efficiency of 92.78% was achieved in 75 minutes while initial pH and current were equal to 3 and 0.5 A respectively. Moreover, COD removal efficiency in slurry reactor was 86.94% which was achieved in 60 minutes once having 0.1 g/L of NZVI concentration and neutral initial pH as components of their optimum parametric condition. In the hybrid system, COD removal efficiency of 93.46% was achieved in only 47 minutes. Energy consumption in hybrid system for achieving the mentioned efficiency was 12.672 KJ which was 40% less than that of single

Electro-Fenton system.

Keywords: advance oxidation; electro-Fenton; petroleum wastewater; energy consumption

Plenary Speech 9: Functional Fabrics with Special Wettabilities

Speaker: Prof. Yan Zhao, College of Textile and Clothing Engineering at Soochow University, China

Time: 16:30-17:15, Tuesday Afternoon, April 23, 2019

Location: Conference Room V (荣泰阁), the 3rd Floor, Ramada Xiamen Hotel I



Abstract

Functional fabrics with special wettabilities including superhydrophobicity, superoleophobicity and stimuli-switchable wettability are useful not only for making technical clothing, such as chemical protective clothes, military uniforms, outdoor sportswear, and soil/stain-resistant clothes for daily use, but also for other applications like oil-water selective adsorption or filtration. This presentation reports our research on fabrication of cotton fabrics with durable superhydrophobicity and pH-induced wettability transition between superhydrophobic and under-water superoleophobic state, as well as polyester fabrics with ammonia-triggered transition from superamphiphobic state to superoleophobic-superhydrophilic state. I will also present our recent research on oleophobic-hydrophilic polyester fabrics and their unique oily stain resistant and release property.

Part III Technical Sessions

Engineering Mathematics and Physics: Plenary Speech II & Technical Session

Session Chair:

Conference Room II (彩虹厅), the 3rd Floor, 14:00-17:00 Tuesday Afternoon, April 23, 2019

Time	Title	Author	Affiliation
14:00-14:45	Performance Analysis of Hopfield Neural Networks as Associative Memory for Fingerprint Images	Dr. Manu Pratap Singh	Dr. B. R. Ambedkar University
14:45-15:30	A model based on fuzzy inference system to analyze the trends of financial market	Dr. Sanjeev Kumar	Dr. B.R. Ambedkar University, Agra
15:30-15:50	NEW FORMULAS FOR THE MAYER AND REE-HOOVER WEIGHTS OF INFINITE FAMILIES OF GRAPHS	Amel Kaouche	Universit éde Moncton
15:50-16:10	Expansion characteristics of a plasma jet in the stepped-wall chamber filled with water	Yi Liu	Nanjing University of Science and Technology
16:10-16:30			
16:30-16:50			
16:50-17:10			
17:10-17:30			

Material, Chemical & Mineral Processing/Metallurgical Engineering:

Technical Session I: Oral Presentations

Session Chair: Dr. Ramesh Subramanian, Laurentian University, Canada

Conference Room V (荣泰阁), the 3rd Floor, 08:30-11:30 Wednesday Morning, April 24, 2019

Paper ID	Title	Author	Affiliation
08:30-08:45	OPTICAL RHEOLOGY OF A VISCOELASTIC SILICONE POLYMER FLUID IN PLANAR EXTENSIONAL FLOW	Ramesh Subramanian	Laurentian University, Canada
08:45-09:00	Fast Activating Persulfate by Crystallization of Fe-based Metallic Glasses with External Energy	Shunxing Liang	Edith Cowan University
09:00-09:15	Characterization of Cooling Rate and Microstructure of Rapidly Solidified Spherical Mono-Sized Sn-1.0Ag-0.5Cu Particles	Yingyan HU	School of Engineering and Technology, China University of Geosciences, China
09:15-09:30	Immobilization of lipase onto magnetic nanoparticles for enantiomer selective acetylation of racemic 1-phenylethylamine	Zhimin Ou	Pharmaceuticals College, Zhejiang University of Technology, China
09:30-09:45	Band Dependent Interlayer f-Electron Hybridization in CeRhIn5	Qiuyun Chen	Science and Technology on Surface Physics and Chemistry Laboratory
09:45-10:00	Stabilizing Cesium Lead Halide Perovskite Lattice through Mn(II) Substitution for Air-Stable Light-Emitting Diodes	Shenghan Zou	Fujian Institute of Research on the Structure of Matter, Chinese Academy of Sciences
10:00-10:15	Low Carbon Steel Foil by asymmetrical rolling	Feng mei Bai	Anhui University of Technology
10:15-10:30	Coffee Break		
10:30-10:45	MnO ₂ /HF/HNO ₃ /H ₂ O System for High-Performance Texturization on Multi-crystalline Silicon	Liu Huan	University of Chinese Academy of Sciences, Beijing 100049, China

10:45-11:00	Numerical and experimental investigations of micromixing performance and efficiency in a pore-array intensified tube-in-tube microchannel reactor	Wenpeng Li	Tianjin University
11:00-11:15	Preparation and Electrochemical Performance of Mg ²⁺ Doped Li ₄ Ti ₅ O ₁₂ Anode Materials for Lithium-Ion Batteries	Ming Wang	Liaoning Technical University
11:15-11:30	Luminous Efficiency of Pd-doped Ag-alloy wire bonded LED Package after Reliability Tests	JUI-HUNG Yuan	Fujian Lightning Optoelectronic Co., Ltd.
11:30-11:45	The Process of Recovering Valuable Metals from Lithium ion Batteries	KAI LUN CHIU	Department of Resources Engineering, National Cheng Kung University, Tainan City, Taiwan
11:45-12:00	Recovery Spent Li-ion Battery by ion-exchange	Kuan-Yu Shih	Department of Resources Engineering, National Cheng Kung University, No.1, University Road, Tainan City, Taiwan
12:00-12:15	Modification of Carbon Nanotubes Microelectrodes in Composite Neural Networks	Wu JiaXi	Institute of Laser Engineering, Beijing University of Technology
12:15-12:30	Fatigue Property of Friction Stir Welded Butt Joints for 6156-T6 Aluminum Alloys	An Chen	Aircraft Strength Research Institute of China, Xi'an, China

Material, Chemical & Mineral Processing/Metallurgical Engineering:

Technical Session II: Poster Presentations

08:30-11:30 Wednesday Morning, April 24, 2019

Paper ID	Title	Author	Affiliation
MST2019_1000 2	Comparative study of calculation methods for shielding thickness of typical materials against gamma rays	Yinghong Zuo	Northwest Institute of Nuclear Technology

MST2019_1010 2	The Microstructure and Solidification Mechanism of Al-Ti-C-Ce Prepared by Petroleum Coke	Xinfeng Zhou	Xijiang China	University,
MST2019_1010 3	Research on TiH ₂ Preparation Mechanism and Structure Properties of Al-Ti-C Mother Alloy.	Xiaoyu Yang	Xijiang China	University,
MST2019_1010 5	Research on the Mechanism and Microstructure of an Al-Ti-C Parent Alloy Prepared Using the Villiaumite–Woodchip Method.	Yu Liu	Xijiang China	University,
MST2019_10111	Effects of Original Microstructure on Hot Deformation Behavior and Microstructure of a p/m Ni-Base Superalloy	Chaoyuan Wang	Science and Technology on Advanced High Temperature Structural Materials Laboratory, Beijing Institute of Aeronautical Materials	
MST2019_10115	Effect of Li ₂ O-Al ₂ O ₃ -Bi ₂ O ₃ -SiO ₂ Glass on Electromagnetic Properties of Ni _{0.16} Cu _{0.22} Zn _{0.62} Fe ₂ O ₄ -BaTiO ₃ Composites at Low Sintering Temperature	Qiang Zhao	State Key Laboratory of Electronic Thin Films and Integrated Devices, University of Electronic Science and Technology of China	
MST2019_2000 2	A Theoretical Investigation on Nonlinear Optical Properties of Organic Substitutions of [Mo ₆ O ₁₉] ²⁻ and [Mo ₇ O ₁₉] ²⁻	Qi Li	Huazhong University of Science and Technology	
MST2019_2000 4	Laminar Flow Characteristics in the Triangular Helical Ducts with Outer Flat Wall	Cuihua Wang	School of Energy and Power Engineering, Shenyang University of Chemical Technology, China	
MST2019_2000 7	Selective oxidation behavior of medium manganese steel in hot-dip galvanizing process	Tong Yang	Shanghai University	
MST2019_2001 0	Effect of intermediate thermomechanical treatment on microstructure and mechanical properties of 2A97 Al-Li alloy	Yu Juan	Beijing Institute of Aeronautical Materials	

MST2019_2001 2	Effects of heat-treatment on microstructures and mechanical properties of hot deformed TiB/Ti-6Al-4V matrix composites	Zhengyang HU	Beijing institute of technology
MST2019_2001 3	Microstructure and mechanical properties of (TiB+ La ₂ O ₃) reinforced titanium matrix composites	Hao Wang	Beijing Institute of Technology
MST2019_2001 4	PMIA/fBN dielectric composite with enhanced breakdown strength and thermal conductivity	Guangyu Duan	Donghua University
MST2019_2001 5	Removal of Trichloroethylene by Corona Radical Injection	Zhan-Guo Li	State Key Laboratory of NBC Protection for Civilian
MST2019_2001 6	High-performance Copolymerized Poly (m-phenylene isophthalamide) (PMIA) Fibers Containing Ether Moiety: Preparation, Structure and Properties	Na Li	State Key Laboratory for Modification of Chemical Fibers and Polymer Materials, Donghua University
MST2019_2001 7	Processing of high purity titanium by equal channel angular pressing at cryogenic temperature	Hongfei Wang	Northeastern University, Shenyang, 110819, Liaoning, China
MST2019_2001 8	Study on the possibility of one-step method processing for PPTA fiber	Xingke Zhang	State Key Laboratory for Modification of Chemical Fibers and Polymer Materials, Donghua University, China
MST2019_2001 9	Modification of UHMWPE fiber by modified nano-graphite in wear resistance	Hongqiu Wang	Donghua University
MST2019_2000 3	Acoustic Emission Study of Fatigue Crack Propagation of Weld Joint for X52 Pipeline Steel	Chang Hong	Industrial training centre, Shenzhen polytechnic, Shenzhen, 518055
MST2019_10116	Improved electrochemical performance of Nd ³⁺ -doped LiNi _{0.5} Mn _{1.5} O ₄ cathode material for 5 V lithium-ion batteries	Aijia Wei	Institute of Energy Resources, Hebei Academy of Science,

			Shijiazhuang 050081, China	Hebei
MST2019_10117	Removal of Alizarin red dye using strong ionization discharge technology	Lanlan Yin	School of the Environment and safety engineering, Jiangsu University, China	
MST2019_10119	Effect of Calcined-bauxite Quality and Secondary Mullitization Reaction on Firing and Properties of Ceramic Plates	Xiao Libiao	College of Materials and Mineral Resources, Xi'an University of Architecture and Technology, Xi'an 710055, China	
MST2019_2000 8	First-principles study on the oxidation mechanism of V alloy surfaces	Xiang Gao	Science and Technology on Surface Physics and Chemistry Laboratory	
MST2019_2002 3	Research on Forming Quality of AlSi10Mg Powder for SLM Process	Dawei Ma	Shanghai Aircraft Design and Research Institute	
MST2019_2002 4	Superhydrophobic Surface Modified by Sol-gel Silica Nanoparticle coating	Xiaoxing Zhang	Soochow University	
MST2019_2002 5	Research on Thermal Aging Characteristics and Mechanism of the Silicon Rubber Insulation Layer of Cable Joints	Yonglan LI	Xi'an Jiaotong University	
MST2019_2004 7	New Strategy for Rapid Detection of the Simulants of Persistent Organic Pollutants Using Gas Sensor Based on 3-D Porous Single-Crystalline ZnO Nanosheets	Hou Nannan	University of Science and Technology of China	
MST2019_2002 8	Modification of Carbon Nanotubes Microelectrodes in Composite Neural Networks	Wu JiaXi	Institute of Laser Engineering, Beijing University of Technology	
MST2019_2003 1	A general and rapid approach to crystalline metal sulfide nanoparticle synthesis for photocatalytic H ₂ generation	Wentao Xu	University of Science and Technology of China	

MST2019_2003 3	Integrated Quasi-Plane Heteronanostructures of MoSe ₂ /Bi ₂ Se ₃ Hexagonal Nanosheets: Synergetic Electrocatalytic Water Splitting and Enhanced Supercapacitor Performance	Jing Yang	University of Science and Technology of China	
MST2019_2003 4	Solution Synthesis of Nonequilibrium Zincblende MnS Nanowires	You Su	University of Science and Technology of China	
MST2019_2003 5	Controlled Construction for Ternary Hybrid of Monodisperse Ni ₃ S ₄ Nanorods/Graphitic C ₃ N ₄ Nanosheets/Nitrogen-Doped Graphene in van der Waals Heterojunctions as Highly Efficient Electrocatalysis for Overall Water Splitting and Promising Anode Material for Sodium-Ion Batteries	Shiqi Xing	University of Science and Technology of China	
MST2019_2003 8	Effective Synthesis of Pb ₅ S ₂ I ₆ Crystals at Low Temperature for Fabrication of High Performance Photodetector	Hongrui Wang	University of Science and Technology of China	
MST2019_2004 3	Effect of Aramid Fiber Surface State on Properties of Epoxy Resin Composites	Manshi Qiu	Xi'an University	Jiaotong
MST2019_2002 1	Refined new technology and application of phosphate rock associated iodine	Jie Zhang	Qiannan University	Normal for Nationalities

Part IV Abstracts

ID: SCET2019_10003

Title: Expansion characteristics of a plasma jet in the stepped-wall chamber filled with water

Name: Yi Liu

Affiliation: Nanjing University of Science and Technology

Email: liuyi61mm@163.com

Abstract:

The interaction mechanism between the plasma and liquid is a key problem for the electrothermal chemical launch technology. To investigate this problem, a simulated experiment for the expansion process of a plasma jet in the working fluid is carried on. Based on this experiment, a two-dimensional axisymmetric unsteady theoretical model is established to reveal the plasma-liquid interaction flow field pattern. The results show that a typical Taylor cavity forms as the plasma jet expands in liquid. The induction effect of the stepped-wall structure enhances the radial expansion of the plasma jet. An arc-shaped pressure wave is generated at the front of the plasma jet and then evolves into the plane wave. A high-pressure area forms at the head of the plasma jet and then moves downstream. There is a strong plasma-liquid turbulent mixing at the interface, especially near the steps and the nozzle exit area.

ID: SCET2019_20007

Title: NEW FORMULAS FOR THE MAYER AND REE-HOOVER WEIGHTS OF INFINITE FAMILIES OF GRAPHS

Name: Amel Kaouche

Affiliation: Université de Moncton

Email: amel.kaouche@umoncton.ca

Abstract:

The virial expansion, in statistical mechanics, makes use of the sums of the Mayer weight of all 2-connected

graphs on n vertices. We study the Mayer weight $w_M(c)$ and the Ree-Hoover weight $w_{RH}(c)$ of a 2-connected graph c which arise from the hard-core continuum gas in one dimension. These weights are computed using signed volumes of convex polytopes naturally associated with the graph c . In the present work, we use the method of graph homomorphisms, to give new formulas of Mayer weights and Ree-Hoover weights for special infinite families of 2-connected graphs.

ID: SCET2019_20008

Title: The Process of Recovering Valuable Metals from Lithium ion Batteries

Name: KAI LUN CHIU

Affiliation: National Cheng Kung University

Email: kelenchiu@gmail.com

Abstract:

The spent Lithium ion Batteries (LIBs) is not only contain valuable metals, such as nickel, cobalt and lithium, but also produce large amounts of metal-containing hazardous waste. Therefore, the development of recycling technologies for spent LIBs has attracted great attention, both for environmental protection and resources conservation.

In this study, we are engaged in developing an effective recycling processes of recovering valuable metal from spent lithium ion batteries. Including reductive roasting technology, reductive acid leaching, ion exchange technology and chemical deposition of cobalt oxalate. The experimental measurements have been made on column chromatography of Ni(II) and Co(II) from solution using DOWEX M4195 as chelating resin and Amberlite IRC 748 as cation exchanger, and also compared the adsorption capacity with other kinds of ion exchange resin, such as S-930, CR-11 and TP-272, to achieve separation and purification of the target metal. Cobalt (II) was then extracted selectively from

the purified aqueous phase. The combined process is simple and adequate for the recovery of valuable metals from spent lithium-ion batteries.

ID: SCET2019_20010

Title: Recovery Spent Li-ion Battery by ion-exchange

Name: Kuan-Yu Shih

Affiliation: National Cheng Kung University

Email: formosa.peter1992@gmail.com

Abstract:

With the vigorous development of 3C products and electric vehicle market, the use of lithium-ion batteries has also increased, and the waste lithium-ion batteries currently recovered in Taiwan have been dealt with outside. There is no resource chemical plant specializing in this battery, so this paper The separation of valuable metals such as nickel, cobalt, lithium and manganese in waste lithium ion batteries was studied, mainly by chemical precipitation combined with ion exchange technology to facilitate the subsequent recovery of raw materials.

The batch process showed that the adsorption process of IRC748 resin was Langmuir thermodynamic model and Pseudo-second order kinetic model. The resin selectivity was $Ni > Co > Mn \gg Li$, and the adsorption of Co and Mn on IRC748 resin was similar. The immersion liquid was adjusted to $pH = 2$, $KMnO_4$ was added to separate the Mn precipitate, and then the liquid phase was partially adjusted to $pH = 4$ to 1.82 BV / hr into the column filled with IRC748 resin for ion exchange reaction to adsorb Co, Ni, and Li exchange. The tail liquid was discharged, and then desorbed with a desorbent $2N\text{ HCl}$ at a flow rate of 0.91 BV / hr . The resulting desorbed solution was adjusted to a concentration of 8 N HCl by concentrated HCl, and then filled with IRA900Cl resin at a flow rate of 1.82 BV / hr . The column is subjected to an ion exchange reaction to adsorb Co, and Ni is discharged with the exchange tail liquid, and then is introduced into the column with a flow rate of 0.91 BV / hr using a desorbent $2N\text{ H}_2\text{SO}_4$,

and the concentration of the Co solution obtained by desorption is 99.97%, and other targets in the Ni solution. The metal concentration is about 2%, and the lithium solution contains almost no other target metal, which has the separation effect of the metal of the lithium ion battery.

ID: MST2019_10000

Title: OPTICAL RHEOLOGY OF A VISCOELASTIC SILICONE POLYMER FLUID IN PLANAR EXTENSIONAL FLOW

Name: Ramesh Subramanian

Affiliation: Laurentian University, Canada

Email: rsubramanian@laurentian.ca

Abstract:

Polymeric macromolecules exhibit isotropic behavior at rest when they are randomly distributed. However, flow deformation causes orientation of the macromolecules leading to anisotropy in the transport properties. Anisotropy to transmission of light by an optical medium produces birefringence, or differences in refractive indices in orthogonal directions. In the case of flexible polymer solutions and melts, the net optical anisotropy caused by flow can be obtained by measuring differences in refractive indices in the direction of the principal stresses. The polarizability tensor ϵ_{ij} via the stress-optical law given by $\epsilon_{ij} = C \sigma_{ij}$ is proportional to the stress tensor σ_{ij} , where C is a material constant known as the stress-optical coefficient. ΔN is the difference in birefringence in any two orthogonal directions, and $\Delta \sigma$ is the difference in the corresponding principal stresses. In this study, the rheology of a viscoelastic polydimethylsiloxane (PDMS) fluid was examined at room temperature for various pressure drops (flow rates) in converging planar extensional flow (a Jeffrey-Hamel type flow) using laser Doppler anemometry (LDA) and birefringence techniques. The first normal stress difference (FNSD) was calculated from the local velocity measurements using the Goddard-Miller model (a quasilinear corotational constitutive equation) with a single Maxwell-type relaxation time constant of 0.0174

s computed from Rouse model (a spring and bead-based network model that describes the conformational dynamics of an ideal chain) and a zero-shear viscosity of 300 Pa.s (obtained from viscometric measurements). The linear relation between the stress and polarizability tensors were confirmed over a range of strain rates that extended well into the non-Newtonian region. A linear stress-optical coefficient of $1.41 \times 10^{-10} \text{ Pa}^{-1}$ was obtained for PDMS in planar extensional flow from birefringence measurements and the first normal stress difference (FNSD) computed using the Goddard-Miller model. This compares well with values for PDMS in the range of $0.909 - 1.84 \times 10^{-10} \text{ Pa}^{-1}$ at room temperature as reported by various researchers. **KEYWORDS:** Polydimethylsiloxane, Flow Birefringence, Stress-Optical Coefficient, Extensional Flow, Goddard-Miller Model, Rouse Model

ID: MST2019_10004

Title: Fast Activating Persulfate by Crystallization of Fe-based Metallic Glasses with External Energy

Name: Shunxing Liang

Affiliation: Edith Cowan University

Email: s.liang@ecu.edu.au

Abstract:

Very recently, crystallization of metallic glasses (MGs) has presented promising properties in the catalytic field. This work has investigated enhanced catalytic performance of crystallized Fe₇₈Si₉B₁₃ ribbons for fast activating persulfate (PS) with assistance of UV-vis light and heat. The ribbons were obtained by annealing at 750°C (Fe-A750) and cibacron brilliant yellow 3G-P (BY 3G-P) dye was used as pollutant. The results indicated that UV-vis light had limited capability to enhance PS activation efficiency by crystallized ribbons while the reaction rate using heat at 65°C was 7.5 times higher than at 25°C, suggesting an advanced performance with heat assistance of Fe-A750 ribbons. Activation energy ΔE for Fe-A750 was measured as 44.5 kJ mol⁻¹. In addition, 5 times reusability could be achieved for Fe-A750 ribbons under 45°C without catalytic decay. The surface morphologies of glassy

ribbons, as-annealed Fe-A750 ribbons, HCl-treated Fe-A750 ribbons and after-reused Fe-A750 ribbons have also been systematically studied. This work provides a novel clue to promote applicability of novel crystallized ribbons from MGs.

ID: MST2019_10106

Title: Characterization of Cooling Rate and Microstructure of Rapidly Solidified Spherical Mono-Sized Sn-1.0Ag-0.5Cu Particles

Name: Yingyan HU

Affiliation: School of Engineering and Technology, China University of Geosciences, Beijing 100083, China

Email: yyhu@ipe.ac.cn

Abstract:

Spherical mono-sized Sn-1.0Ag-0.5Cu (wt.%) particles with diameter ranging from 124.0 to 337.4 μm were prepared by the pulsed orifice ejection method (termed "POEM"). These spherical Sn-1.0Ag-0.5Cu particles exhibit a good spherical shape and a narrow size distribution, suggesting that liquid Sn-1.0Ag-0.5Cu can completely break the balance between the surface tension and the liquid static pressure in the crucible micropores and accurately control the volume of the droplets. Furthermore, the relationship between cooling rate and microstructures of spherical Sn-1.0Ag-0.5Cu particles was studied with a specific focus on different particle diameter during the rapid solidification. The cooling rate of spherical Sn-1.0Ag-0.5Cu particles with different diameter was evaluated by the Newton's cooling model. It is revealed that the cooling rate decreases gradually with the increase of particle size during the rapidly solidified process. When the particle diameter is equal to 75 μm, the cooling rate of the Sn-1.0Ag-0.5Cu particle achieves $4.30 \times 10^3 \text{ K/s}$ which indicates that smaller particles can rapidly solidified due to their higher cooling rate. Meanwhile, the cooling rate decreases rapidly when the particle diameter increases between 75 and 100 μm. Furthermore, the different particle diameter with different cooling rate has a great influence on the solidification

microstructure of Sn-1.0Ag-0.5Cu particles. The cooling rate and grain boundary size decreases with the increase of particle diameter during the rapid solidification. In addition, the phase size of β Sn increases with the decrease of particle size. Smaller particles have relatively high cooling rate and it gives less solidification time as compared to larger particles. It is an effective route for fabrication of high-quality spherical Sn-1.0Ag-0.5Cu particles

ID: MST2019_20006

Title: Immobilization of lipase onto magnetic nanoparticles for enantiomer selective acetylation of racemic 1-phenylethylamine

Name: Zhimin Ou

Affiliation: Pharmaceuticals College, Zhejiang University of Technology, Hangzhou, Zhejiang, 310014, China

Email: oozmm@163.com

Abstract:

Abstract: In this study, magnetic chitosan microspheres (Fe₃O₄-CTS) were prepared via chemical co-precipitation and cross-linked with lipase using glutaraldehyde to form Fe₃O₄-CTS-glutaraldehyde-lipase particles. The textural characteristics of Fe₃O₄-CTS-glutaraldehyde-lipase particles were assessed by scanning electron microscopy. The optimal immobilization conditions were 2.1 mg/mL lipase, 10 mg/mL Fe₃O₄-CTS-glutaraldehyde, pH 7.5, 30 °C, 2 h. The immobilization efficiency was 53% and the amount of lipase was 111.3 mg/g carrier. Fe₃O₄-CTS-glutaraldehyde-lipase particles was used in resolution of racemic 1-phenylethylamine in a solvent-free system. The conversion, enantiomeric excess of (R)-N-(1-phenylethyl)acetamide, and E value reached 33.6%, 97%, and 107 respectively.

ID: MST2019_20011

Title: Band Dependent Interlayer f-Electron Hybridization in CeRhIn₅

Name: Qiuyun Chen

Affiliation: Science and Technology on Surface Physics and Chemistry Laboratory

Email: sheqiuyun@126.com

Abstract:

A key issue in heavy fermion research is how subtle changes in the hybridization between the 4f (5f) and conduction electrons can result in fundamentally different ground states. CeRhIn₅ stands out as a particularly notable example: when replacing Rh with either Co or Ir, antiferromagnetism gives way to superconductivity. In this photoemission study of CeRhIn₅, we demonstrate that the use of resonant angle-resolved photoemission spectroscopy with polarized light allows us to extract detailed information on the 4f crystal field states and details on the 4f and conduction electron hybridization, which together determine the ground state. We directly observe weakly dispersive Kondo resonances of f electrons and identify two of the three Ce 4f_{15/2} crystal-electric-field levels and band-dependent hybridization, which signals that the hybridization occurs primarily between the Ce 4f states in the CeIn₃ layer and two more three-dimensional bands composed of the Rh 4d and In 5p orbitals in the RhIn₂ layer. Our results allow us to connect the properties observed at elevated temperatures with the unusual low-temperature properties of this enigmatic heavy fermion compound.

ID: MST2019_02004

Title: Stabilizing Cesium Lead Halide Perovskite Lattice through Mn(II)

Substitution for Air-Stable Light-Emitting Diodes

Name: Shenghan Zou

Affiliation: Fujian Institute of Research on the Structure of Matter, Chinese Academy of Sciences

Email: zoushenghan@fjirsm.ac.cn

Abstract:

All-inorganic cesium lead halide perovskite (CsPbX₃, X = Cl, Br, and I) quantum dots (QDs), possessing high photoluminescence quantum yields and tunable color

output, have recently been endowed great promise for high-performance solar cells and light-emitting diodes (LEDs). Although moisture stability has been greatly improved through separating QDs with a SiO₂ shell, the practical applications of CsPbX₃ QDs are severely restricted by their poor thermal stability, which is associated with the intrinsically low formation energies of perovskite lattices. In this regard, enhancing the formation energies of perovskite lattices of CsPbX₃ QDs holds great promise in getting to the root of their poor thermal stability, which hitherto remains untouched. Herein, we demonstrate an effective strategy through Mn²⁺ substitution to fundamentally stabilize perovskite lattices of CsPbX₃ QDs even at high temperatures up to 200 °C under ambient air conditions. We employ first-principle calculations to confirm that the significantly improved thermal stability and optical performance of CsPbX₃:Mn²⁺ QDs arise primarily from the enhanced formation energy due to the successful doping of Mn²⁺ in CsPbX₃ QDs. Benefiting from such an effective substitution strategy, these Mn²⁺-doped CsPbX₃ QDs can function well as efficient light emitters toward the fabrication of high-performance perovskite LEDs.

ID: MST2019_20009

Title: Low Carbon Steel Foil by asymmetrical rolling

Name: Feng mei Bai

Affiliation: Anhui University of Technology

Email: baifengmei@ahut.edu.cn

Abstract:

At room temperature, the low carbon steel were cold rolled from 0.5 mm to 1 μm without intermediate annealing by asymmetrical rolling (ASR) process. the microstructure were investigate by Electron Backscatter Diffraction (EBSD) and transmission electron microscopy (TEM). Lath structure (~300 nm) and local nanograins (~60nm) were obtained through ASR with extensibility up to 50,000%. The high angle boundaries were predominant. The results indicated that inhomogeneous deformation and combination

deformation mechanism of dislocation slip and grain boundary slip in the foil ASR process.

ID: MST2019_20029

Title: Preparation and Electrochemical Performance of Mg²⁺ Doped Li₄Ti₅O₁₂ Anode Materials for Lithium-Ion Batteries

Name: Ming Wang

Affiliation: Liaoning Technical University

Email: mawang.lntu@hotmail.com

Abstract:

Spinel Li₄Ti₅O₁₂ (LTO) doped with Mg²⁺ was synthesized by solid-phase reaction method. The Mg²⁺ doping quantity was 3%, 6%, 9%, and 12%, respectively. The structure and electrochemical performance of the prepared LTO composites were investigated by XRD, SEM, Electrochemical Impedance Spectroscopy (EIS), and galvanostatic charge-discharge tests. It was found that the doped Mg ion did not change the structure of Li₄Ti₅O₁₂, and it was evenly distributed around Li₄Ti₅O₁₂. When Mg²⁺ doping quantity increased from 3% to 12%, the internal resistance and charge transfer resistance of the composite both decreased. The first discharge specific capacity of 6%-Mg²⁺ doped LTO composite was 168 mAh/g, which was close to the theoretical capacity of pure lithium titanate (175 mAh/g), and the capacity retention rate was 98% after 100 cycles.

ID: MST2019_20020

Title: MnO₂/HF/HNO₃/H₂O System for High-Performance Texturization on Multi-crystalline Silicon

Name: Liu Huan

Affiliation: University of Chinese Academy of Sciences, Beijing 100049, China

Email: liuhuan@mail.iee.ac.cn

Abstract:

It was found that the addition of MnO₂ particles into the HF/HNO₃/H₂O system could significantly improve the

texturization etching performance on multi-crystalline silicon (mc-Si) wafer. For a wide component ratio range of HF/HNO₃/H₂O from HF-rich to HNO₃-rich, by optimizing the MnO₂ usage and the etching time, the addition of MnO₂ particles always reduced the texture reflectance greatly. Low weighted average surface reflectance (Ra) for the AM1.5G sun spectrum in the wavelength range of 380–1100 nm was achieved on both the slurry wire sliced (SWS) mc-Si and the diamond wire sliced (DWS) mc-Si. Due to its excellent effect and simple processing, the MnO₂/HF/HNO₃/H₂O etching system can be expected as a candidate for high-performance texturization on mc-Si wafer, especially on DWS mc-Si wafer.

ID: MST2019_10107

Title: Fatigue Property of Friction Stir Welded Butt Joints for 6156-T6 Aluminum Alloys

Name: An Chen

Affiliation: Aircraft Strength Research Institute of China, Xi'an, China

Email: andychen1986@163.com

Abstract:

This study was conducted to investigate fatigue behavior of friction stir welding (FSW) butt joints for 6156-T6 aluminum alloy. The detail fatigue rating (DFR) values of 6156-T6 FSW joints is obtained based on statistical analysis of fatigue tests. The micrographs of weld structure were observed by optical microscope (OM), Fatigue fractography was researched under scanning electron microscope (SEM). The results indicate that DFR value of 6156-T6 FSW joints is 153.31MPa. Fatigue property of FSW butt joints is sensitive to the microstructural features, such as nugget zone (NZ), thermo mechanically affected zone (TMAZ) and heat affected zone (HAZ). The hardness distributions of the FSW joints reveal W-shaped profiles. Fractography shows that fatigue cracking is initiated at weak-bonding defects, which are located at the root site of the butt joint. The weak-bonding defects have obvious influence on the fatigue properties of friction stir welding.

ID: MST2019_10002

Title: Comparative study of calculation methods for shielding thickness of typical materials against gamma rays

Name: Yinghong Zuo

Affiliation: Northwest Institute of Nuclear Technology

Email: zuoyhnint@163.com

Abstract:

The paper aims to analyze the shielding ability of concrete and lead material to gamma rays at different energies, and the relationships between the shielding thickness of the two materials and energy of gamma ray and attenuation factor are obtained by using the method of attenuation multiple and method of half-value-thickness, respectively. The results show that when the energy of gamma ray and attenuation factor are determined, the thickness of the concrete shield layer obtained by the method of attenuation multiple is greater than that obtained by the half-value-thickness method. For lead materials, the relative magnitude of thicknesses of lead shield obtained by the method of attenuation multiple and the method of half-value-thickness method are related to the energy of gamma rays. When the gamma ray energy is lower than 8 MeV, the thickness of lead shield calculated by the method of attenuation multiple is larger than that obtained by the half-value-thickness method, while when the gamma ray energy is higher than 8 MeV, the conclusion is opposite.

ID: MST2019_10102

Title: The Microstructure and Solidification Mechanism of Al-Ti-C-Ce Prepared by Petroleum Coke

Name: Xinfeng Zhou

Affiliation: Xijiang University, China

Email: hydongq@126.com

Abstract:

The microstructure of an Al-Ti-C-Ce alloy was studied

by XRD, SEM, and EDS. This mother alloy consisted of $\alpha(\text{Al})$, (AlTi) , (TiC) , and $(\text{Ti}_2\text{Al}_{20}\text{Ce})$ phases, and there was a second phase of a composite structure. The TiC phase was the primary crystal nucleus, and the (TiAl) phase was segregated on the surface to form a $\text{TiC}-(\text{TiAl})$ composite crystal nucleus. Al formed a fine $\text{TiC}-(\text{TiAl})-\alpha(\text{Al})$ primary composite crystal nucleus by a peritectic reaction. The primary composite crystal nucleus with higher energy and larger cluster size was taken as the core, and other composite crystal nuclei were segregated on its surface to form a secondary composite crystal nucleus. Next, the secondary composite crystal nucleus formed the tertiary composite crystal nucleus, and so on, to form the titanium-enriched area of composite particles.

ID: MST2019_10103

Title: Research on TiH₂ Preparation Mechanism and Structure Properties of Al-Ti-C Mother Alloy.

Name: Xiaoyu Yang

Affiliation: Xijiang University, China

Email: zhouxinfeng1993@163.com

Abstract:

Structure properties of Al-Ti-C mother alloy which was prepared by TiH_2 and graphite method were studied by various characterization methods. Results demonstrated that the synthesis process of Al-Ti-C alloy contained three stages. Firstly, TiH_2 and graphite was respectively used as titanium and carbon sources. Secondly, titanium reacted with aluminum and graphite, producing Ti-Al , C-Al , Ti-C compounds. Finally, these compounds formed Al-Ti-C alloy. It was equiaxed or dendrite structure with grain size of $20 \sim 40 \mu\text{m}$. There were needle-like and elongated phases in alloy matrix. There are petal primary crystals containing Ti , C , Fe and Si on grain boundaries. Ti and C distribute evenly along grain boundaries and grains. Ti and C enrichment and segregation occurred close to the primary phase. Cryolites were conducive to wetting of carbon and aluminum, the second phase generated more fully in the grain.

ID: MST2019_10105

Title: Research on the Mechanism and Microstructure of an Al-Ti-C Parent Alloy Prepared Using the Villiumite–Woodchip Method.

Name: Yu Liu

Affiliation: Xijiang University, China

Email: yangxiaoyu19930706@163.com

Abstract:

X-ray diffraction, scanning electron microscopy, energy dispersive spectroscopy, differential scanning calorimetry, and thermogravimetric analysis were used to study the microstructure and properties of an Al-Ti-C parent alloy prepared using the villiumite–woodchip method. The synthesis process of the Al-Ti-C parent alloy prepared using the villiumite–woodchip method and aluminum liquid had the following stages: The first stage was the formation of titanium aluminum by titanium being displaced from the reaction between aluminum and villiumite. The second stage was the dehydration and carbonization reactions of the woodchips at high temperatures. The third stage involved titanium aluminum, carbon aluminum, and titanium carbon compounds constitute the Al-Ti-C parent alloy with a refined effect water and carbon dioxide, which were the cracking products of the woodchips, reacted with aluminum to produce alumina and hydrogen, which accumulated in the grain boundary in the form of slag-gas pockets.

ID: MST2019_10111

Title: Effects of Original Microstructure on Hot Deformation Behavior and Microstructure of a p/m Ni-Base Superalloy

Name: Chaoyuan Wang

Affiliation: Science and Technology on Advanced High Temperature Structural Materials Laboratory, Beijing

Institute of Aeronautical Materials

Email: wchy2005@126.com

Abstract:

The hot deformation behavior and microstructure of a powder metallurgy (P/M) Ni-base superalloy with different original microstructure were studied by isothermal compression tests. The isothermal compression tests were conducted on Gleeble-3500D simulator with the temperature range of 1000°C~1100°C and the strain rate of 0.001s⁻¹~0.1s⁻¹. The results showed that the flow stress of the specimens with fine grains (10µm) and ultrafine grains (3µm) gained by hot extruding (HEX) were much less than the that with the average grain diameter of 30µm by hot isostatic pressing (HIP). At the strain rate of 0.001s⁻¹, the as-HIPed specimens with the average grain diameter of 30µm showed steady-state deformation at 1100°C only, whereas the as-HEXed specimens with the average grain diameter of 10µm and 3µm showed steady-state deformation both at 1050°C and 1100°C. The flow stress showed decreasing trend as the average grain diameter decreasing. The activation energy of hot deformation decreased from 622.79 kJ mol⁻¹ to 302.36 kJ mol⁻¹ as the average grain diameter decreased from 30µm to 3µm. When the as-HEXed specimen with the average grain diameter of 3µm was deformed at the condition of (1050°C, 0.001s⁻¹), the flow stress was lower than that at the condition of (1100°C, 0.001s⁻¹), and the former also gained much finer and uniform grain, the later gained mixed grains.

ID: MST2019_10115

Title: Effect of Li₂O-Al₂O₃-Bi₂O₃-SiO₂ Glass on Electromagnetic Properties of Ni_{0.16}Cu_{0.22}Zn_{0.62}Fe₂O₄-BaTiO₃ Composites at Low Sintering Temperature

Name: Qiang Zhao

Affiliation: State Key Laboratory of Electronic Thin Films and Integrated Devices, University of Electronic Science and Technology of China

Email: qzh@uestc.edu.cn

Abstract:

In the present work, the composite material Ni_{0.16}Cu_{0.22}Zn_{0.62}Fe₂O₄-BaTiO₃ (NCZF-BTO, in a 10:1) was synthesized with different additive

amounts of Li₂O-Al₂O₃-Bi₂O₃-SiO₂ (LABS) glass using a traditional solid-state reaction method and sintered at 900 °C. The synthesized composites were then comparatively investigated; in addition to their phases and density, their magnetic and dielectric properties, which include the saturation magnetization(4πMs), coercivity (H_c), permeability (μ'), quality factor (Q), dielectric constant (ε') and dielectric loss (tan δ) were characterized. In contrast to the undoped composites, the performance of the LABS-doped samples were enhanced. The optimal performance was obtained when the LABS glass content reached 1.0wt%. At this level of doping, the bulk density increased from 4.883 g/cm³ to 5.021g/cm³, the saturation magnetization (4πMs) increased from 3819.5 to 4113.6Gs, the coercivity (H_c) decreased from 111 to 106.5A/m, the permeability (μ') at 10 MHz increased from 25.8 to 61.1, and the dielectric constant (ε') at 10 MHz increased from 18.9 to 23.4. On further increasing the LABS glass content to 1.5 wt%, the performance of the composite generally deteriorated, except for the dielectric constant, which increased to 27.1. In short, the optimal LABS glass doping ratio was determined to be 1.0 wt%

ID: MST2019_20002

Title: A Theoretical Investigation on Nonlinear Optical Properties of Organic Substitutions of [Mo₆O₁₉]²⁻ and [Mo₇O₁₉]²⁻

Name: Qi Li

Affiliation: Huazhong University of Science and Technology

Email: liqi_hust@hust.edu.cn,363482924@qq.com

Abstract:

In this study, density functional theory (DFT) was used to calculate second-order polarizabilities densities of a series of organic substitution for Lindqvist-type polyoxometalates (POMs), and the nonlinear optical (NLO) properties was also analyzed. We found that β_{zzz} has the main contribution to β value. The expansion of molecular structure on z-axis greatly increased second-order polarizabilities. Both the size of

the organic segments and metal hybridization exert an influence on β value. The analysis on the second-order polarizabilities density is used to explain the NLO phenomenon. In the present investigation, metal hybridization and π -conjugation changed the contribution of β_{zzz} value from different parts. The results of this work will contribute to the potential applications in high-performance NLO materials.

ID: MST2019_20004

Title: Laminar Flow Characteristics in the Triangular Helical Ducts with Outer Flat Wall

Name: cuihua Wang

Affiliation: School of Energy and Power Engineering, Shenyang University of Chemical Technology, China

Email: wch-7855@163.com

Abstract:

A hydrodynamically fully developed laminar flow in the triangular helical duct with outer flat wall is numerically studied in this work. The numerical program code in terms of vorticity, stream function and axial velocity component under the orthogonal helix coordinate system is written on account of a finite volume method. The flow fields of the triangular helical ducts with outer flat wall are given, the effects of Dean and the curvature ratio on flow resistance are observed. The results show that the secondary flow pattern is found to be changed from two vortices to four vortices when the Dean number increases, and the critical Dean number is about 108. As Dean and Prandtl numbers increasing, the flow resistance increase sharply, especially when Dn rises to 108 from 107.

ID: MST2019_20007

Title: Selective oxidation behavior of medium manganese steel in hot-dip galvanizing process

Name: Tong Yang

Affiliation: Shanghai University

Email: shumailyangt@shu.edu.cn/13061980090@163.com

Abstract:

Surface oxides of medium manganese steel treated under different hot-dip galvanizing processes were analyzed by X-ray photoelectron spectroscopy, scanning electron microscope microscopy and energy dispersive spectrometer techniques. Combined with thermodynamic calculation, the effects of dew point, annealing temperature and alloying elements on the formation of oxides were investigated. It was shown that many oxides such as Cr_2O_3 and Al_2O_3 , which deteriorate galvanizing performance largely, were formed at lower dew point, and that the formation of Cr and Al oxides could be effectively inhibited at higher dew point. It was also shown that higher annealing temperature weakened the galvanizing performance because of the formation of harmful oxides on the surface of the experimental steel; the formation of MnO could be controlled by regulating the rate of Al/Mn in the composition of experimental steel, thus reducing the surface defect.

ID: MST2019_20010

Title: Effect of intermediate thermomechanical treatment on microstructure and mechanical properties of 2A97 Al-Li alloy

Name: Yu Juan

Affiliation: Beijing Institute of Aeronautical Materials

Email: yuer1437@126.com

Abstract:

Effect of intermediate thermomechanical treatment on tensile properties at short-transverse direction, fracture mechanism and microstructure of 2A97 Al-Li alloy thick plate were studied by tensile testing, SEM, EBSD and TEM. The results show that with the increasing of compression deformation, the strength and elongation of the alloy increase first and then decrease slightly. The fracture mode of the alloy changes from quasi-cleavage fracture to high energy ductile fracture. When the compression deformation rises to 20%, the elongated structure are replaced by a more uniform and equiaxial structure. The distribution of phase distribute more homogeneously in the grains.

ID: MST2019_20012

Title: Effects of heat-treatment on microstructures and mechanical properties of hot deformed TiB/Ti-6Al-4V matrix composites

Name: Zhengyang HU

Affiliation: Beijing institute of technology

Email: Huzy_job@163.com

Abstract:

In this paper, TiB reinforced Ti-6Al-4V matrix composites were successfully fabricated using a spark plasma sintering, hot rolling and heat treating process. (transformed β -Ti + secondary α -Ti) domains were formed in TiB/TMCs after heat treatment. The size of these domains increases from 2.5 μm to 4.6 μm with the increase of solution time. The aspect ratio of whiskers monotonously decreases along with the solution time extending. The highest ultimate tensile strength of 1332 MPa and yield-strength of 1315 MPa were achieved by (940 $^{\circ}\text{C}$, 15min+ water-quenching+537 $^{\circ}\text{C}$, 4h) TMC.

ID: MST2019_20013

Title: Microstructure and mechanical properties of (TiB+ La₂O₃) reinforced titanium matrix composites

Name: Hao Wang

Affiliation: Beijing Institute of Technology

Email: 2320710394@qq.com

Abstract:

Titanium alloys are widely applied in aerospace, military, automotive and petrochemical engineering owing to the specific mechanical properties. However, the development of traditional titanium alloys has become increasingly unable to meet the growing demand for comprehensive material properties. The mechanical properties of the titanium alloys cannot be significantly improved by changing the internal structure, such as changing or adding solid solution elements, or changing the heat treatment process. By adding the reinforcing phase to prepare a

titanium-based composite material, it is possible to utilize the enhanced phase to optimize the composite structure, which has become an important development direction for improving the performance of titanium alloys. The titanium matrix composites reinforced with high aspect ratio TiB whiskers (TiBw) and nanometer sized La₂O₃ which using micron-sized LaB₆ and Ti-6Al-4V materials as raw material, have been synthesized by spark plasma sintering (SPS) technique and heat treatment (HT). The results show that the in-situ formed La₂O₃ particles are diffusely distributed in the matrix and the maximum aspect ratio of TiBw is 25 which is much higher than traditional ways. Besides, with the increasing volume fraction of TiB, the strength of the titanium matrix composites increases and the ductility is decreased. The reinforcing phases show a good reinforcement effect and the strengthening effects of matrix strengthening, load-bearing effect of TiBw as well as the dispersion strengthening are also studied.

ID: MST2019_20014

Title: PMIA/fBN dielectric composite with enhanced breakdown strength and thermal conductivity

Name: Guangyu Duan

Affiliation: Donghua University

Email: duanguangyu1991@126.com

Abstract:

A high-temperature poly(m-phenyleneisophthalamide) (PMIA) dielectric composite was successfully manufactured with functionalized BN (fBN) fillers. Due to effective modification by KH-550, fBN particles evenly dispersed in PMIA matrix. The dielectric property, breakdown strength and thermal conductivity of PMIA/fBN dielectric composite were researched. The consequences indicate that fBN fillers can not only decrease the dielectric loss but also enhance the breakdown strength of PMIA/fBN dielectric composites. Furthermore, owing to the generated heat transfer pathways by fBN particles, the thermal conductivities improved from 0.23 W m⁻¹ K⁻¹ of fBN-0 to 0.86 W m⁻¹ K⁻¹ of fBN-30, demonstrating a

significant improvement. These results present a novel method for fabricating high-temperature PMIA/fBN dielectric composites with improved breakdown strength and thermal conductivity.

ID: MST2019_20015

Title: Removal of Trichloroethylene by Corona Radical Injection

Name: Zhan-Guo Li

Affiliation: State Key Laboratory of NBC Protection for Civilian

Email: lizg618@126.com

Abstract:

The removal of trichloroethylene (TCE) by corona discharge plasma was investigated. The influences of initial concentration, gas flow rate, injection of water vapor and O₃ on removal efficiency were discussed. The results show that removal efficiency reduces with the initial concentration and gas flow rate increasing. A proper quantity of water vapor injection can improve the removal efficiency, but which is not always increased, due to the electronegative characteristic of water molecule. The maximum removal efficiency of 90.7% can be obtained in wet air flow with relative humidity of 70.6%. The removal efficiency increases obviously with O₃ injection. The decomposition products are CHCl₂COCl, COCl₂, HCl and CO₂, based on which the decomposition mechanism is discussed. The oxygen chain reaction is the primary decomposition mechanism, and high energy electrons and active oxygen species play a leading role in the decomposition process. Therefore, removal efficiency of TCE can be improved greatly when water vapor and O₃ is injected.

ID: MST2019_20016

Title: High-performance Copolymerized Poly (m-phenylene isophthalamide) (PMIA) Fibers Containing Ether Moiety: Preparation, Structure and Properties

Name: Na Li

Affiliation: State Key Laboratory for Modification of Chemical Fibers and Polymer Materials, Donghua University

Email: lina0607email@163.com

Abstract:

Copolymerized poly (m-phenylene isophthalamide) (co-PMIA) fibers with excellent thermal stability and good mechanical properties were developed via solution polycondensation process based on m-phenylenediamine (MPD), isophthaloyl dichloride (IPC), and 3,4'-oxydianiline (3,4'-ODA). Effects of the ether moiety on the structure and properties of the copolymers were investigated. A series of co-PMIA nascent fibers were produced using wet-spinning method. The coagulation process to form co-PMIA nascent fibers were studied by examination of SEM and strength tester. The co-PMIA nascent fibers with the MPD/3,4'-ODA molar ratio of 8:2 showed an optimum dye uptake.

ID: MST2019_20017

Title: Processing of high purity titanium by equal channel angular pressing at cryogenic temperature

Name: Hongfei Wang

Affiliation: Northeastern University, Shenyang, 110819, Liaoning, China

Email: wanghf_neu@163.com

Abstract:

Experiments show that high purity titanium (HP-Ti) samples have been successfully processed by equal channel angular pressing (ECAP) using a 120 degree die and a relatively slow ram speed at cryogenic temperature when the HP-Ti rods were trapped with 6061 Al alloy tubes. Optical microscopy (OM) and transmission electron microscopy (TEM) were utilized to investigate the deformed microstructure of the material. Typical microstructures of shear bands and deformation twinning were found in the deformed microstructure of ECAPed HP-Ti. Furthermore, the SAED pattern analysis of the twinning structures revealed that the deformation twinning occurred on

{11 22} planes.

ID: MST2019_20018

Title: Study on the possibility of one-step method processing for PPTA fiber

Name: Xingke Zhang

Affiliation: State Key Laboratory for Modification of Chemical Fibers and Polymer Materials, Donghua University, 201620, Shanghai, China

Email: zhangxingke2015@163.com

Abstract:

In this paper, the low molecular weight poly(p-phenylene terephthalamide) (LMW-PPTA) solutions with different end group were obtained through changing molar ratio of monomers. Then, the high molecular weight PPTA (HMW-PPTA) polymer was synthesis by Secondary copolymerization. At that time, the PPTA fiber may be produced by means of reaction spinning in one step. Hence, the possibility of one-step method processing for PPTA fiber was studied by investigating the polymerization degree and gelling time of secondary copolymerization under different situations. The one-step method processing for PPTA fiber is not only free from the dependence on concentrated sulfuric acid, but also able to be controllable easily. Remarkably, the facile procedure, lower cost and better environmental protection are significant for the manufacture of PPTA fiber.

ID: MST2019_20019

Title: Modification of UHMWPE fiber by modified nano-graphite in wear resistance

Name: Hongqiu Wang

Affiliation: Donghua University

Email: whq134@126.com

Abstract:

Single UHMWPE fiber was modified by modified NG in wear resistance. Wear resistance, tensile strength, TGA were used to characterize the effect of modified NG on the properties of UHMWPE fiber. The results

showed that with the increasing content of modified NG, the wear resistance of UHMWPE fiber was enhanced and its tensile strength was decreased. Considering the tensile strength and wear resistance of fiber, the optimum content of modified NG in UHMWPE fiber was around 0.58%. At this content, the wear resistance of UHMWPE fiber was increased 1.88 times than pure UHMWPE fiber.

ID: MST2019_20003

Title: Acoustic Emission Study of Fatigue Crack Propagation of Weld Joint for X52 Pipeline Steel

Name: Chang Hong

Affiliation: Industrial training centre, Shenzhen polytechnic, Shenzhen, 518055

Email: hchang@szpt.edu.cn

Abstract:

The crack propagation of different weld joint samples, which were from the basic metal, weld seam and heat affected zone (HAZ), were detected by acoustic emission (AE) technique. The results showed that the crack growth rate of basic metal was higher than weld seam and HAZ because of the transverse compressive residual stress in joint. But the coarse of grains was the reason for higher rate of weld seam than that of HAZ. And AE waveforms of crack propagation from three microstructures were different. The most compositions of AE signals were higher frequency of 300KHz for weld seam and lower one of 100KHz for basic metal and HAZ.

ID: MST2019_10116

Title: Improved electrochemical performance of Nd³⁺-doped LiNi_{0.5}Mn_{1.5}O₄ cathode material for 5 V lithium-ion batteries

Name: Aijia Wei

Affiliation: Institute of Energy Resources, Hebei Academy of Science, Shijiazhuang Hebei 050081, China

Email: weiaijia2012@126.com

Abstract:

Spinel powders of Nd-doped $\text{LiNi}_{0.5}\text{Nd}_x\text{Mn}_{1.5-x}\text{O}_4$ with different Nd^{3+} contents ($x = 0, 0.01, \text{ and } 0.02$) have been synthesized by a solid-state ball milling method. The samples were characterized by XRD, SEM and EDS. XRD shows the doping of Nd^{3+} did not destroy the formation of spinel LNMO. The results show that $\text{LiNi}_{0.5}\text{Nd}_{0.01}\text{Mn}_{1.49}\text{O}_4$ sample exhibits a higher rate performance with specific discharge capacities of 134.8, 137.2, 136.5, 130.4, 123.8, 106.4, and 83.1 mAh g^{-1} at 0.2, 0.5, 1, 2, 3, 5, and 7 C (1 C = 140 mAh g^{-1}), respectively. The results indicate that the Nd^{3+} doping could reduce the electrode polarization and enhance the rate capacities.

ID: MST2019_10117

Title: Removal of Alizarin red dye using strong ionization discharge technology

Name: Lanlan Yin

Affiliation: School of the Environment and safety engineering, Jiangsu University, China

Email: lanlanyin1995@163.com

Abstract:

The degradation of Alizarin red dye (Anthraquinone) was investigated using a novel technique of strong ionization discharge to generate high oxidation active species from oxygen. Under the optimum conditions, AR dye was almost removed with degradation rate reaching 95%, by radicals such as $\bullet\text{OH}$ and O_3 generated within the strong ionization discharge reactor. The intermediate products were analyzed by ultraviolet (UV) spectroscopy, total organic carbon (TOC) analysis, liquid chromatography-mass spectrometry (LC-MS) and ion chromatography (IC) to validate the degradation efficiency of the strong ionization discharge for AR dye and to deduce its possible decomposition pathway. Finally, it has been confirmed that the sulfur element on AR molecule results into sulfate, an environmentally friendly substance. This work shows that the strong ionization discharge can efficiently be used for the degradation of Anthraquinone dyes as well as other extensively used

textile dyes.

ID: MST2019_10119

Title: Effect of Calcined-bauxite Quality and Secondary Mullitization Reaction on Firing and Properties of Ceramic Plates

Name: Xiao Libiao

Affiliation: College of Materials and Mineral Resources, Xi'an University of Architecture and Technology, Xi'an 710055, China

Email: 584957167@qq.com

Abstract:

Addition of different types of calcined bauxites to the ceramic plate formulation was performed to study effects on the firing and properties of the resulting ceramic plates. The physical and chemical characteristics, high-temperature reaction degree, thermochemical behavior, mineral composition, and microstructure of the calcined bauxites were analyzed. The results showed that lightly calcined bauxite could minimize the linear shrinkage rate. However, incomplete high-temperature secondary mullitization reaction could inhibit completion of product sintering and result in a loose microstructure, high water absorption index, and low modulus of rupture. Application of super calcined bauxite yielded a product with good sintering performance and low water absorption; increased amounts of mullite reinforcement phase also increased the strength of the plate. The degree of secondary mullitization was the main factor affecting the performance of the ceramic plate.

ID: MST2019_20008

Title: First-principles study on the oxidation mechanism of V alloy surfaces

Name: Xiang Gao

Affiliation: Science and Technology on Surface Physics and Chemistry Laboratory

Email: gaoliang_198521@163.com

Abstract:

Vanadium alloys are promising structural materials for

advanced fusion reactors because of their low activation characteristics and excellent high temperature mechanical properties. However, vanadium alloys have high hydrogen permeability owing to their high hydrogen solubility, which is detrimental to structural materials. The use of a layer named hydrogen permeation barrier (HPB) is an effective way to reduce the hydrogen isotopes penetration. Aluminum rich coatings, with α -Al₂O₃ scale on the surface, are identified as the best solution. Such aluminum rich coatings are usually formed by aluminizing and subsequent selective oxidation. One of the greatest challenges is how to realize selective oxidation of Al to form a dense alumina scale. The experimental results indicated that, for V-30 vol.%Al alloys, the formed oxides were composed of V₂O₅ and Al₂O₃. The alloys exhibit improved oxidation resistance by adding Ti (or Cr), yet the oxide scale still comprise a mixture of V₂O₅, Al₂O₃, and TiO₂ (or Cr₂O₃). To reveal the microscopic mechanism for oxidation of V alloys and to predict selective oxidation of V alloys, we have investigated the oxidation behaviors of V alloys and constructed surface phase diagrams (SPDs) for oxygen adsorption on V-X(110) (X=Ti, Al or Cr) alloy surfaces by first-principles DFT calculations. Based on the calculated SPDs, for V-Ti and V-Al alloys, the formed oxides should comprise mixture of V oxides and TiO₂ (or Al₂O₃); while for V-Cr alloys, the formed oxides should be V oxides only. The analysis provides an explanation for the experimental oxidation behaviors of V alloys.

ID: MST2019_20023

Title: Research on Forming Quality of AlSi10Mg Powder for SLM Process

Name: Dawei Ma

Affiliation: Shanghai Aircraft Design and Research Institute

Email: madawei@comac.cc

Abstract:

In order to study the forming quality of AlSi10Mg powder for SLM process without supporting structure,

as well as lay the foundation of subsequent structural design of Aluminum SLM technique, a series of typical coupons have been designed and printed. Based on comprehensive consideration of layout direction, overhang angle, hole size, etc., Xline 2000R with optimized process parameter has been used as SLM equipment for AlSi10Mg powder. Through the analysis of printed coupons, the beneficial conclusion is made which can be used to guide future design, especially for the structure with complex shape.

ID: MST2019_20024

Title: Superhydrophobic Surface Modified by Sol-gel Silica Nanoparticle coating

Name: xiaoxing zhang

Affiliation: Soochow University

Email: 1015190605@qq.com

Abstract:

We reported a superhydrophobic silica-coated surface with a water contact angle of 160° with a 4 μ L water droplet, and transparency of 70-86% in the wavelength range of 380-800 nm. The silica film was synthesized at room temperature (22 °C) using sol-gel process by a simple, cost-effective and uniform spin-coating by mixing silicon dioxide sol-gel with γ -(2,3-epoxypropyloxy) propyltrimethoxysilane (KH-560). The durability of the coating could be effectively enhanced by controlling the ratio of KH-560 and modified silicon dioxide sol-gel. It was believed that this process that we used can hold a great potential in super-hydrophobic surface fabrication.

ID: MST2019_20025

Title: Research on Thermal Aging Characteristics and Mechanism of the Silicon Rubber Insulation Layer of Cable Joints

Name: Yonglan LI

Affiliation: Xi'an Jiaotong University

Email: 1920381680@qq.com

Abstract:

In order to solve the thermal aging problem of silicone rubber insulation layer of 220 kV integral prefabricated cable joints, the mass loss and thermal gravimetric (TG) were tested, the change of the mass loss rate and thermal stability of silicone rubber insulation layer in the thermal aging process at different temperature and time were investigated. The thermal aging mechanism of thermal degradation reaction of silicone rubber molecular chains was analyzed by gel content test and infrared spectrum test (IR). The results showed that the thermal degradation reactions mainly occurred in the silicone rubber insulation sample during the thermal aging process. The cross-linked network of the molecular chain structure gradually deteriorates, resulting in the increase of mass loss rate and the decrease of thermal stability, and the increase of dual peak of differential thermal weight (DTG), the decrease of initial decomposition temperature and the remaining mass. With increasing aging temperature and aging time, the aging would be accelerated. These properties could reflect the degree of thermal aging of silicone rubber insulation layer. The results could also provide theoretical support for the preparation, operation and maintenance for silicone rubber cable joints.

ID: MST2019_20047

Title: New Strategy for Rapid Detection of the Simulants of Persistent Organic Pollutants Using Gas Sensor Based on 3-D Porous Single-Crystalline ZnO Nanosheets

Name: Hou Nannan

Affiliation: University of Science and Technology of China

Email: hounan@mail.ustc.edu.cn

Abstract:

It is significant to detect the persistent organic pollutants (POPs) in an environment for both human health and environmental risk assessment. However, most of the current analytical techniques require complicated and tedious processes and are time consuming. Semiconducting metal-oxide sensors are predominant solid-state gas detecting devices for

domestic, commercial, and industrial application. Here, combining both the advantages of instrument analytical methods and the metal-oxide sensors, a gas chromatography column was placed in front of a metal-oxide sensor to separate POP simulants from a mixture. The metal-oxide sensor was used to detect the separated sample. To improve the sensitivity, 3D porous single-crystalline ZnO nanosheets (PSCZNs) were synthesized by a one-pot hydrothermal method followed by an annealing treatment. Then, the as-prepared 3D PSCZN-based sensors were exploited to couple with gas chromatography column. The simulants of POPs were used to assess the as-prepared sensor and chromatography column coupled measurement method. The experiment results showed a promise for rapid detection of POPs by metal-oxide sensors.

ID: MST2019_20028

Title: Modification of Carbon Nanotubes Microelectrodes in Composite Neural Networks

Name: Wu JiaXi

Affiliation: Institute of Laser Engineering, Beijing University of Technology

Email: 791105368@qq.com

Abstract:

In order to improve the conductivity of carbon nanotube microelectrodes in composite neural networks, Graphenenanoribbons(GNRs) formed by excimer laser (150-550 mJ) irradiation dissociation of carbon nanotubes. The morphology of the GNRs was observed by scanning electron microscopy (SEM), and the properties of graphene were characterized by Raman spectroscopy. Finally, the conductivity of the microelectrodes was measured by a semiconductor parameter measurement system. Laser energy and irradiation time are two important parameters for the preparation of graphene from carbon nanotubes. Raman spectroscopy shows that the Raman characteristics of graphene characterized by optimized process are enhanced. At the same time, the scanning electron microscopy (SEM) results show that the bonding effect and surface morphology of carbon nanotubes (CNTs) are also changed, which has an important influence on

the conductivity of microelectrodes. The results show that when the laser energy is 150 mJ, the carbon nanotubes are not opened, and the connection of carbon nanotubes can be observed. When the laser energy is 450 mJ, carbon nanotubes can be destroyed effectively and graphene bands can be partially opened. At this time, the conductivity of the electrode is the best. At the same time, due to the thermal accumulation effect, a large number of holes appear on the tube wall at 550 mJ. Key words: excimer laser, Carbon nanotubes, Graphenenanoribbons, Micromorphology, Electrical characteristics

ID: MST2019_20031

Title: A general and rapid approach to crystalline metal sulfide nanoparticle synthesis for photocatalytic H₂ generation

Name: Wentao Xu

Affiliation: University of Science and Technology of China

Email: 1421121572@qq.com

Abstract:

Herein, we report a facile and rapid dry route rather than a solution process to prepare crystalline CdS nanoparticles via microwave-assisted thermolysis of a Cd-thiourea complex. CdS prepared by 35 min microwave heating offers a H₂ generation rate of 103.2 mmol/h that is comparable to the H₂ generation rate of commercially available CdS (96.3 mmol/h). Importantly, the present synthetic strategy can be generalized to prepare other metal sulfides, including ZnS and MoS₂, and ZnS–CdS solid solutions

ID: MST2019_20033

Title: Integrated Quasi-Plane Heteronanostructures of MoSe₂/Bi₂Se₃ Hexagonal Nanosheets: Synergetic Electrocatalytic Water Splitting and Enhanced Supercapacitor Performance

Name: Jing Yang

Affiliation: University of Science and Technology of China

Email: yjing@mail.ustc.edu.cn

Abstract:

MoSe₂ as one of typical transition metal dichalcogenides holds great potential for energy storage and catalysis while its performance is largely limited by its poor conductivity. Bi₂Se₃ nanosheets, a kind of topological insulator, possess gapless edges on boundary and show metallic character on surface. According to the principle of complementarity, we designed a novel integrated quasi-plane structure of MoSe₂/Bi₂Se₃ hybrids with artistic heteronanostructures via a hot injection in colloidal system. Interestingly, the heteronanostructures are typically constituted by single-layer Bi₂Se₃ hexagonal nanoplates evenly enclosed by small ultrathin hierarchical MoSe₂ nanosheets on the whole surfaces. XPS investigations suggest obvious electron transfer from Bi₂Se₃ to MoSe₂, which could help enhance the conductivity of the hybrid electrode. Especially, schematic energy band diagrams derived from UPS studies indicate that Bi₂Se₃ has higher EF and smaller Φ than MoSe₂, further confirming the electronic modulation between Bi₂Se₃ and MoSe₂, where Bi₂Se₃ serves as an excellent substrate to provide electrons and acts as channels for high-rate transition. The MoSe₂/Bi₂Se₃ hybrids demonstrate a low onset potential, small Tafel slope, high current density and long-term stability suggests the excellent hydrogen evolution reaction activity whereas a high specific capacitance, satisfactory rate capability and rapid ions diffusion indicates the enhanced supercapacitor performance.

ID: MST2019_20034

Title: Solution Synthesis of Nonequilibrium Zincblende MnS Nanowires

Name: You Su

Affiliation: University of Science and Technology of China

Email: yousu@mail.ustc.edu.cn

Abstract:

Uniform four-coordinate nonequilibrium MnS nanowires mainly in zincblende structure, other than the stable rock-salt phase, are reported for the first time. The MnS nanowires are grown via a solution–solid–solid model from the reaction of a Mn(II) source with dibenzyl disulfide in oleylamine at 180–200 °C catalyzed by Ag₂S nanocrystals in a body-centered cubic (bcc) fast-ionic phase transformed from their low-temperature monoclinic form. Investigations show that most of the zincblende MnS nanowires are grown along the $\langle 112 \rangle$ zone axis but a small proportion grow along the $\langle 111 \rangle_{\text{ZB}} / \langle 0001 \rangle_{\text{Wur}}$ axis with zincblende/defect-section and/or wurtzite/defect-section superlattices connected with the stems along the $\langle 112 \rangle$ direction. The nanowires have a tendency to grow straight at relatively low reaction temperature for short reaction times but twist at high temperature for long reaction times. Meanwhile, relatively high temperatures and long times favor the transition of the MnS nanowires in the zincblende phase to the corresponding thermodynamic ones in rock-salt form. Interestingly, even small increases in reaction pressure (1–2 atm) sensitively influence the growth of the MnS nanowires from zincblende to wurtzite form in the present catalytic system although low-pressure changes commonly do not have an obvious effect on condensed matter. In addition, the optical and magnetic properties of the zincblende MnS nanowires were studied, and they are varied largely from the bulk

ID: MST2019_20035

Title: Controlled Construction for Ternary Hybrid of Monodisperse Ni₃S₄ Nanorods/Graphitic C₃N₄ Nanosheets/Nitrogen-Doped Graphene in van der Waals Heterojunctions as Highly Efficient Electrocatalysis for Overall Water Splitting and Promising Anode Material for Sodium-Ion Batteries

Name: Shiqi Xing

Affiliation: University of Science and Technology of China

Email: xingsq@mail.ustc.edu.cn

Abstract:

As a kind of novel multi-functional nanocomposites, ternary hybrid of monodisperse Ni₃S₄ nanorods/graphitic C₃N₄ nanosheets/nitrogen-doped graphene with heterostructured architecture is controllably constructed for the first time, which illustrates great potential for overall water splitting and fabrication of sodium-ion battery. Intensive investigations revealed that the ternary hybrid with robust and intertwined nanostructures possesses shorter diffusion pathways, smaller diffusion resistance and faster transfer speed of electrons and ions that could expedite transport of electrolyte to flood and interact with reaction sites, dynamically and thermodynamically. Notably, the active Ni₃S₄ nanorods within the unique integrated ternary hybrid as embedded in graphitic C₃N₄ nanosheets over a conducting substrate of nitrogen-doped graphene could avoid agglomeration, obscission, anisotropic volume expansion and irreversible mechanical failure intensively even during extreme electrochemical reactions. Owe to the integrated effect, the ternary hybrid delivers excellent electrochemical performances with long-term stability in water splitting and cyclic durability in sodium-ion battery. Especially, there is a low onset potential of 40 mV (vs RHE, $J = -1.5 \text{ mA cm}^{-2}$) to be observed in HER process, and the applied potentials are also conducted as small as 1.47 V (vs RHE) and 1.51 V for OER and overall water splitting, respectively, at a 10 mA cm⁻² under the same alkaline conditions. As for sodium-ion battery, the ternary hybrid possesses an advanced specific capacity of ~670 mAh g⁻¹ at 100 mA g⁻¹ with particularly excellent rate capability and could even work at a high current density.

ID: MST2019_20037

Title: Luminous Efficiency of Pd-doped Ag-alloy wire bonded LED Package after Reliability Tests

Name: JUI-HUNG Yuan

Affiliation: Institute of Materials Science and Engineering, National Taiwan University, Taiwan
Fujian Lightning Optoelectronic Co., Ltd.

Email: rayyuan@tdled.com

Abstract:

In this study, binary Ag-alloy wires were doped with different Pd concentrations, and each wire was encapsulated in an LED package. The initial optical characteristics were tested, and reliability was tested with the high temperature storage life (HTSL), high temperature operating life (HTOL) and wet high temperature operating life (WHTOL). The luminous efficiency of the Ag-alloy wire LED package was about 2% higher than that of the Au wire package, but the addition of 6% Pd to the Ag-alloy wire decreased the luminous efficiency to close to that of the Au-wire LED package. This was due to the high reflectivity of silver in the blue wavelength region, as compared to the low reflectivity of palladium. After 1,000 hours of HTOL and WHTOL, the results showed that the performance of luminous flux maintenance increased with increasing Pd content, indicating that Ag-alloy wires doped with a sufficient amount of Pd can inhibit degradation due to oxidation reaction and thermal and humidity aging. Therefore, binary Ag-Pd alloy wires produced with specific drawing and annealing processes are suitable for mid-power white light LEDs in lighting applications.

ID: MST2019_20038

Title: Effective Synthesis of Pb₅S₂I₆ Crystals at Low Temperature for Fabrication of High Performance Photodetector

Name: Hongrui Wang

Affiliation: University of Science and Technology of China

Email: whr@mail.ustc.edu.cn

Abstract:

Sulfoiodide crystal possesses promising properties and functionalities that would be used for technical applications in many areas. In this work, high-quality rod-like lead sulfoiodide (Pb₅S₂I₆) crystals with about 3-mm long have been synthesized via a rapid hydrothermal process at temperature low down to 160 °C for 10 h with the assistance of acid media (hydrochloride acid). The structure of the Pb₅S₂I₆

crystals is characterized, and the optical property of the crystals is measured and investigated based on the first-principles density functional theory (DFT) calculations. Meanwhile, the photoresponse performance of the Pb₅S₂I₆ crystal to white light is studied for the first time, typically using an individual Pb₅S₂I₆ crystal constructed on SiO₂/Si substrate. This photodetector shows a fast and sensitive response with a rise/decay time of less than 0.2 s and a high on-off photoswitching ratio of 650. The responsivity of the device is 0.567 mA W⁻¹, the detectivity is 2.69 × 10⁹ Jones and the noise equivalent power (NEP) is 4.08 × 10⁻¹³ W Hz^{-1/2}.

ID: MST2019_20043

Title: Effect of Aramid Fiber Surface State on Properties of Epoxy Resin Composites

Name: Manshi Qiu

Affiliation: Xi'an Jiaotong University

Email: qms2017@stu.xjtu.edu.cn

Abstract:

The surface state of aramid fiber was modified by coupling agent to characterize the change of surface state of aramid fiber. The fiber / epoxy resin composites were prepared to study the mechanical and electrical properties and the internal mechanism of how different surface states affect. The results show that, after the treatment with the coupling agent, the surface roughness of the aramid fiber is increased and the surface activity is enhanced. At the same time, the coupling agent treatment of the aramid fiber makes the interface state with the epoxy resin significantly improved, and the mechanical and electrical properties of the composites further improved.

ID: MST2019_20021

Title: Refined new technology and application of phosphate rock associated iodine

Name: Jie Zhang

Affiliation: Qiannan Normal University for Nationalities

Email: 15929725636@163.com

Abstract:

Iodine associated with phosphate rock is an important part of iodine resources, thus technology development and comprehensive utilization of recycling and refining of iodine associated is significant. From the process of phosphate rock processing recycling $\omega < 95\%$ of the crude iodine need refined into a w of 99.5% or more pure iodine. This paper briefly introduces the phosphate rock associated iodine recycling method, is described in detail sublimation method refining technology and operation method of the iodine analyzes the problems existing in the production and puts forward corresponding solving measures.

ID: MST2019_02011

Title: Numerical and experimental investigations of micromixing performance and efficiency in a pore-array intensified tube-in-tube microchannel reactor

Name: Wenpeng Li

Affiliation: Tianjin University

Email: 1126587187@qq.com

Abstract:

A new kind of pore-array intensified tube-in-tube microchannel reactor (PA-TMCR) was constructed and studied to achieve intensive micromixing performance as well as high throughput but low pressure drop. The Villermaux–Dushman reaction was employed to investigate the micromixing performance with different geometric structures and flow conditions. A Finite-rate/Modified eddy dissipation model (FR/MEDM) was improved with a correlated mixing rate A at the range of $Re=485\sim 5308$ to build the mixing model. Both results indicated that the pore size and annular size played a significant role in enhancing the micromixing level, and the design of PA-TMCR should avoid the overlap of flow fields from the adjacent pores and too much pressure-drop in the annular. The micromixing time was estimated with incorporation model and a total energy efficiency was proposed to evaluate the energy efficiency of the whole reactor. The optimal micromixing time and total energy efficiency could reach 0.06 ms and 9.0% in PA-TMCR. The comparison with other reactors shows that the PA-TMCR is an efficient and high throughput reactor to meet the industrial applications with excellent micromixing performance and total energy efficiency.

Keywords: PA-TMCR; Finite-rate/Modified eddy dissipation model; Micromixing performance; Total energy efficiency.

Part V Instructions for Presentations

Oral Presentation

Devices Provided by the Conference Organizing Committee:

- Laptops (with MS-office & Adobe Reader)
- Projectors & Screen
- Laser Sticks

Materials Provided by the Presenters:

- PowerPoint or PDF files

Duration of each Presentation:

- Regular Oral Session: 15-20 Minutes of Presentation
- Plenary Speech: 40-50 Minutes of Presentation

Poster Presentation

Materials Provided by the Conference Organizing Committee:

- X Racks & Base Fabric Canvases (60cm×160cm, see the figure below)
- Adhesive Tapes or Clamps

Materials Provided by the Presenters:

- Home-made Posters

Requirement for the Posters:

- Material: not limited, can be posted on the Canvases
- Size: smaller than 60cm×160cm
- Content: for demonstration of the presenter's paper



Part VI Hotel Information

About Hotel

Ramada Xiamen Hotel (厦门华美达长升大酒店) Ramada Hotel Xiamen is located at the golden area of Xiamen Island, quite near to local government and shopping center, Cultural Arts Center, and the well-known scenic spots, such as Gulang Islet and Nan Pu Tuo Temple. It takes no more than 15 minutes for a taxi to reach the hotel from both the international airport and the Exhibition Center. The advantage of location brings about the convenience of transportation as well as apropos environment. We are committed to provide careful and thoughtful care experience for each guest in every moment.

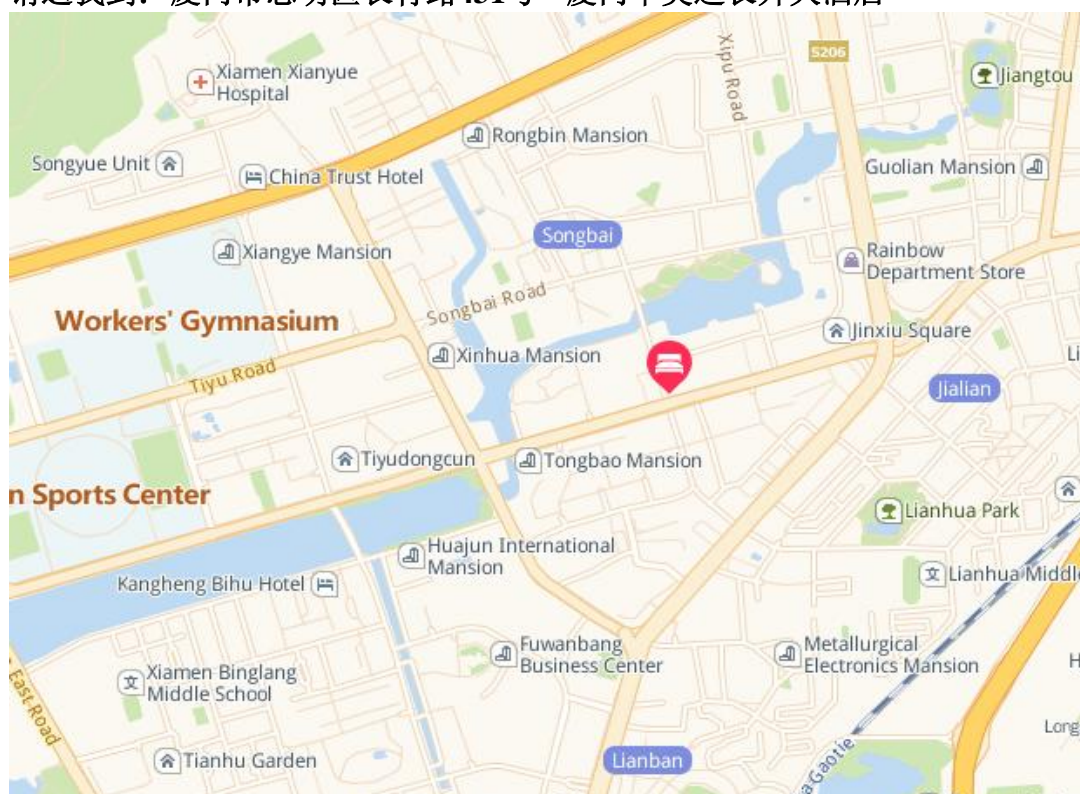
Address: No.431, Changqing Road, Xiamen, China
(厦门市思明区长青路431号)

URL: <http://5850.hotel.cthy.com/>

Telephone: + 86 592 5031333

Fax: + 86 592 5030303

For non-Chinese author, please show the following info to the driver if you take a taxi:
请送我到：厦门市思明区长青路431号 厦门华美达长升大酒店



Transportation

Gaoqi International Airport 9.27km

Xiamen Railway Station 4.03km

Xiamen North Railway Station 20.38km

Contact Us

Organizing Committee

Secretary: Ms. Rolin

Email: scet@engii.org/ scet_service@163.com

Tel: +86 151 7233 0844

QQ: 741494290; 3025797047

WeChat: 3025797047

Linkedin: SCET Conference